Self-triggered Coverage Control for Mobile Sensors

Erick J. Rodríguez-Seda, Xiaotian Xu, Josep M. Olm, Arnau Dòria-Cerezo, and Yancy Diaz-Mercado

***Abstract*—The deployment and coordination of mobile sensor networks for coverage control applications can present several practical challenges including how to efficiently share limited communication resources and how to reduce the use of localization devices (e.g., radars and lidars). One potential solution to these challenges is to reduce the frequency at which agents communicate or sample each other's position. In this paper, we present a distributed, asynchronous self-triggered control policy for centroidal Voronoi coverage control that is shown to decrease the sampling or communication instants among agents without degrading the performance of the mobile sensor network. Each agent independently decides when to sample the position of nearby agents and uses outdated information of its neighbors until new information is required. We prove that the locational cost function describing the distribution of agents monotonically decreases everywhere outside of a bounded neighborhood around the group's optimal configuration and that the agents asymptotically converge to their Voronoi centroids if the data-sampled centroid errors approach zero. In addition, we show that the sampling intervals are always positive and lower bounded and, as illustrated by simulations and experiments, they tend to stabilize at a large value as the mobile sensor network comes to a steady-state. Simulations and experiments with ground vehicles validate the proposed control strategy and show that the proposed policy can achieve similar level of performance as a continuous or fast periodic implementation.**

I. Introduction

The use of mobile sensors for area coverage control has gained considerable attention in the last two decades [1]. The objective of coverage control is to spatially distribute a group of mobile sensors in a task domain such that the entire space is sampled or monitored while optimizing the collective sensing capability of the network. Applications include surveillance [2], force protection [3], public safety [4], positioning service [5], and environmental sampling [6].

Several frameworks have been proposed for area coverage control (refer to [1], [7] for topical reviews). The work presented in this paper will focus on computational geometry-based algorithms that employ Voronoi partitions [8]–[10] for static coverage using mobile robots with isotropic sensors (or communication range). Other effective coverage control policies include potential field methods [11], path planning algorithms [12], grid-based controllers [13], [14], awareness-based models [15], [16], cooperative swarm-based approaches [17], statistical methods [18], persistent control [16], [19], [20], and game theoretical strategies [21], [22]. Despite the coverage control strategy, a common assumption among distributed policies is the use of continuous or periodic communication (or localization) among sensors (also termed as agents) in order to complete the coordination task [23]. The latter may not only be impractical, but it may also deplete energy resources at a faster rate [24] and cause delays and data collisions in the communication network [1]. One solution to reduce the use of communication or localization sensors, such as radars and lidars, is to implement event-based control strategies [25]. An event-based control strategy is one that requests or sends new information based on the occurrence of an event, which is the case of event-triggered control; or the prediction of such event, which is known as self-triggered control [26]. For example, in [27] the authors applied an asynchronous error-driven strategy to a coverage control problem that uses estimates of other agents' positions between samplings to compensate for the lack of up-to-date information. However, a convergence analysis using the position estimates is not provided. Similarly, in [28] an event-triggered control using the coverage control framework of [8] is proposed. The control law is shown to drive the agents to a Centroidal Voronoi Tessellation (CVT) and to avoid Zeno behavior (i.e., communication intervals are lower bounded) if the velocities of the centroids are bounded.

Event-triggered strategies can reduce the instants in which the controller is updated but still requires agents to continuously communicate or monitor the position of nearby agents at all times. To overcome the shortcomings of event-triggered control, one may opt for a self-triggered implementation [29]. A self-triggered implementation determines when new information is needed based on the neighbors' last available information. The authors of [30] proposed a self-triggered coverage control policy based on [8] that is guaranteed to achieve similar convergence properties as a continuous implementation. This work was later extended with concepts of event-triggered control by communicating *velocity promises* among agents aimed to attenuate the increase of communication instants once the network is converging to a CVT [31] and to $k-$coverage applications where k number of agents are required to cover every point in the domain [32]. An interesting work by the same research group is also presented in [33] where an event-triggered broadcasting approach is proposed. Each agent is responsible to decide when to broadcast (rather than request) its position to other agents in a bounded vicinity. The implementation succeeds in decreasing the communication instants by reducing the communication frequency and eliminating message requests but, similar to [30], the communication frequency tends to increase once the mobile sensor network approaches a CVT.

This work was supported in part by the Office of Naval Research Grant No. N0001419WX01589, by the Government of Spain through the Agencia Estatal de Investigación Project No. DPI2017-85404-P, and by the Generalitat de Catalunya through the AGAUR Project No. 2017 SGR 872.

E. J. Rodríguez-Seda is with the Department of Weapons, Robotics, and Control Engineering at the United States Naval Academy, Annapolis, MD (email: rodrigue@usna.edu).

X. Xu and Y. Diaz-Mercado are with the Department of Mechanical Engineering at the University of Maryland, College Park, MD (e-mail: xxu0116@umd.edu; yancy@umd.edu).

J. M. Olm and A. Doria-Cerezo are with the Institute of Industrial and Control Engineering at the Polytechnic University of Catalonia, Spain (e-mail: josep.olm@upc.edu; arnau.doria@upc.edu).

In this paper, we present a distributed, asynchronous self-triggered coverage control policy based on Lloyd's algorithm [8] that is shown to 1) reduce the inter-agent sensing (or communication) frequency and 2) locally optimize the position of an arbitrarily large group of mobile sensors by approaching a CVT. The control strategy exploits the concepts of guaranteed [34] and dual guaranteed Voronoi cells [30] and uses a conservative prediction-based formulation of self-triggered control [35] to determine the next sampling or sensing instant with negligible impact on the locational cost. The main highlights and differences with respect to previous work can be summarized as follows:

- We show that the communication intervals are always lower bounded by a positive constant regardless of the configuration and, in contrast to previous related work, we provide closed-loop formulas to compute these bounds whenever the agents satisfy a minimum separation distance.
- We provide bounds on the change of mass for the guaranteed and dual guaranteed Voronoi cells within sensing (or communication) instants.
- Similar to [30] and [33], the proposed self-triggering rule uses an estimate of the upper bound on the Voronoi centroid error to dictate when new information is required. However, in contrast to [30] and [33] which use constant inputs between sensing intervals, the proposed formulation uses bounded, piece-wise continuous state-feedback control inputs and a different triggering condition that takes also into consideration the size of the guaranteed Voronoi cells. We then show that the proposed bounded linear control input locally minimizes the locational cost function under some mild assumptions.
- Different from [30] and [33], the proposed self-triggered control strategy tends to reduce the sensing frequency (i.e., increases the time intervals between the sensing of nearby agents position) when the mobile sensor network converges to a CVT. In particular, the control update algorithm in [30] approaches the fast sampling implementation of a continuous control policy when reaching a CVT.
- In contrast to [33], which requires agents to broadcast their coordinates and velocity promises, our approach requires the acquisition of only position information which can be obtained by onboard proximity sensors that can detect the relative position of nearby agents. In addition, the event-triggered strategy of [33] continuously (or periodically) evaluates a triggering condition, whereas the proposed self-triggered control only evaluates the triggering condition at each irregular sensing (or communication) instant.
- We present simulation and experimental results with ground vehicles that validate the scalability, convergence, and communication advantages of the proposed self-triggered control policy.

II. Preliminaries

Let $\mathbb{R}^n$, $\mathbb{R}_{\geq 0}$, and $\mathbb{Z}_{\geq 0}$ represent the sets of all n-dimensional real vectors, all non-negative real numbers, and all non-negative integers, respectively. We denote the Euclidean norm of a vector $\mathbf{x} \in \mathbb{R}^n$ as $\|\mathbf{x}\|$ and the closed n-dimensional ball centered at $\mathbf{x}$ with radius $r \in \mathbb{R}_{\geq 0}$ as $\mathcal{B}[\mathbf{x}, r] := \{\mathbf{y} \in \mathbb{R}^n \mid \|\mathbf{x} - \mathbf{y}\| \leq r\}$. We define the surface area and volume of $\mathcal{B}[\mathbf{x}, r]$ as $\mathcal{A}_n(r)$ and $\mathcal{V}_n(r)$, respectively. Furthermore, we denote the boundary of a set S as ∂S and its diameter as $\mathrm{dm}(S) = \sup_{\mathbf{x},\mathbf{y} \in S} \|\mathbf{x} - \mathbf{y}\|$.

A. Static Coverage Problem

Consider a group of N mobile sensors with Cartesian position denoted by $\mathbf{p}_i \in \mathbb{R}^n$, $\forall\ i \in \mathbb{N} := \{1, \cdots, N\}$. The agents are tasked with sensing (i.e., covering) a convex, compact domain $\mathbb{Q} \subset \mathbb{R}^n$. It is assumed that information about the task domain does not change over time and that the task can ultimately be solved using a static configuration of agents, that is, the task is to find the optimal fixed location for a set of agents [15]. Furthermore, we will assume each agent's position evolves according to the following equation

$$\dot{\mathbf{p}}_i(t) = \mathbf{u}_i(t) \tag{1}$$

where $\mathbf{u}_i(t) \in \mathbb{R}^n$ denotes the control input.

A common solution to optimize the configuration of agents for static coverage is to minimize a locational cost function $\mathcal{H}$ of the form [8]

$$\mathcal{H}(\mathbb{P}(t)) = \sum_{i \in \mathbb{N}} \int_{V_i(\mathbb{P}(t))} f(\|\mathbf{q} - \mathbf{p}_i(t)\|)\phi(\mathbf{q}) d\mathbf{q} \tag{2}$$

where $\mathbb{P}(t) := (\mathbf{p}_1(t), \cdots, \mathbf{p}_N(t))$ and $V_i(\mathbb{P}(t)) \subset \mathbb{Q}$ denote the regions of dominance (with disjoint interiors) that each ith sensor needs to cover. The term $f : \mathbb{R}_{\geq 0} \to \mathbb{R}_{\geq 0}$ is a differentiable, monotonically increasing function measuring the sensing performance degradation of the ith sensor, whereas the continuous differentiable distribution density function $\phi : \mathbb{Q} \to \mathbb{R}_{\geq 0}$ captures the importance of covering a particular point $\mathbf{q} \in \mathbb{Q}$. Herein, we will assume that $f(\|\mathbf{q} - \mathbf{p}_i(t)\|) = \|\mathbf{q} - \mathbf{p}_i(t)\|^2$, similar to [8], and that $\phi(\mathbf{q}) \in [\phi_{\min}, \phi_{\max}]$ for some $0 < \phi_{\min} \leq \phi_{\max} < \infty$ and $\forall\ \mathbf{q} \in \mathbb{Q}$.

A well known necessary condition for the minimization of (2) is that $V(\mathbb{P}(t)) := \{V_1(\mathbb{P}(t)), \cdots, V_N(\mathbb{P}(t))\}$ is a Voronoi partition of $\mathbb{Q}$, i.e.,

$$V_i(\mathbb{P}(t)) = \{\mathbf{q} \in \mathbb{Q} \mid \|\mathbf{p}_i(t) - \mathbf{q}\| \leq \|\mathbf{p}_j(t) - \mathbf{q}\|\ \forall\ j \neq i\}$$

and that $\mathbb{P}(t)$ forms a CVT [8], [36]. Note that $V_i(\mathbb{P}(t))$ can be interpreted as the set of points $\mathbf{q} \in \mathbb{Q}$ that are closer or equidistant to $\mathbf{p}_i(t)$ than any other agent. By CVT it is meant that $\mathbf{p}_i(t) = \mathbf{c}_{V_i}(t)\ \forall\ i \in \mathbb{N}$, where $\mathbf{c}_{V_i}(t)$ is the centroid of the ith Voronoi cell. In general, the centroid $\mathbf{c}_S$ and mass m_S of a set $S \subset \mathbb{Q}$ can be computed as

$$\mathbf{c}_S = \frac{\int_S \mathbf{q}\phi(\mathbf{q}) d\mathbf{q}}{m_S}, \qquad m_S = \int_S \phi(\mathbf{q}) d\mathbf{q}. \tag{3}$$

One approach to achieve a CVT is to apply Lloyd's method. In [37] it is shown that if the agents positions evolve according to the continuous-time Lloyd's descent algorithm

$$\dot{\mathbf{p}}_i(t) = \mathbf{u}_i(t) = \kappa(\mathbf{c}_{V_i}(t) - \mathbf{p}_i(t)) \tag{4}$$

where $\kappa > 0$ is a proportional gain, the multi-agent configuration asymptotically converges to a CVT under some mild assumptions. Lloyd's method has the advantage of being distributed given that computations of $\mathbf{c}_{V_i}(t)$ only depend on position information of the ith agent's Voronoi neighbors. We say that the jth sensor is a Voronoi neighbor of the ith agent if V_i and V_j share an edge (i.e., $\partial V_i \cap \partial V_j \neq \emptyset$), denoted as ∂V_{ij}, and define the set of indexes of the ith agent's neighbors at time t as $\mathbb{N}_i(t)$. The cardinality of these neighbor sets is known to be bounded, on average. For instance, the average of Voronoi neighbors per agent does not exceed six if $\mathbb{Q} \subset \mathbb{R}^2$ [38].

Remark 1: It is worth mentioning that for any pair $(\mathbb{Q}, \phi)$ there are in general multiple CVTs and that Lloyd's method (4) can only guarantee convergence of $\mathcal{H}(\mathbb{P}(t))$ to a local minimum [8].

B. Static Coverage Problem with Position Uncertainty

The above definitions of a Voronoi cell and centroid require accurate position information from all neighbors. In the case that there is uncertainty on the position of agents, it is convenient to introduce the concepts of guaranteed [34] and dual guaranteed Voronoi cells [30].

Let $\mathbb{D}_i \subset \mathbb{Q}$ represent the uncertainty on the ith agent location, i.e., $\mathbf{p}_i(t) \in \mathbb{D}_i$, and $\mathbb{D} := \{\mathbb{D}_1, \cdots, \mathbb{D}_N\}$ denote the set of uncertainties for all agents. The ith guaranteed Voronoi cell, $gV_i(\mathbb{D})$, is the set of points $\mathbf{q} \in \mathbb{Q}$ that are guaranteed to be closer or equidistant to the ith agent than any other agent and is defined as

$$gV_i(\mathbb{D}) = \{\mathbf{q} \in \mathbb{Q} | \max_{\mathbf{x} \in \mathbb{D}_i} \|\mathbf{x} - \mathbf{q}\| \leq \min_{\mathbf{y} \in \mathbb{D}_j} \|\mathbf{y} - \mathbf{q}\| \ \ \forall\ j \neq i\}.$$

In general, the set $gV(\mathbb{D}) := \{gV_1(\mathbb{D}), \cdots, gV_N(\mathbb{D})\}$ is not a partition of $\mathbb{Q}$ and $gV_i(\mathbb{D})$ are disjoint and convex sets.

Complementary to the concept of guaranteed Voronoi cell, the ith dual guaranteed Voronoi cell, $dgV_i(\mathbb{D})$, is defined as

$$dgV_i(\mathbb{D}) = \{\mathbf{q} \in \mathbb{Q} | \min_{\mathbf{x} \in \mathbb{D}_i} \|\mathbf{x} - \mathbf{q}\| \leq \max_{\mathbf{y} \in \mathbb{D}_j} \|\mathbf{y} - \mathbf{q}\| \ \ \forall\ j \neq i\}$$

and the points $\mathbf{q} \in \mathbb{Q}$ outside of $dgV_i(\mathbb{D})$ denote the set of points that are guaranteed to be closer or equidistant to some agent other than the ith sensor. The set $dgV(\mathbb{D}) := \{dgV_1(\mathbb{D}), \cdots, dgV_N(\mathbb{D})\}$ is a cover but not a partition, in general, of $\mathbb{Q}$ and $dgV_i(\mathbb{D})$ may be concave and overlap. Note that by definition one has that $gV_i(\mathbb{D}) \subseteq V_i(\mathbb{P}(t)) \subseteq dgV_i(\mathbb{D})$ $\forall\ i \in \mathbb{N}$. If there is no uncertainty on the agents location, i.e., $\mathbb{D} = \mathbb{P}(t)$ are single points, then, $gV_i(\mathbb{D}) = V_i(\mathbb{P}(t)) = dgV_i(\mathbb{D})$ $\forall\ i \in \mathbb{N}$. Fig. 1 illustrates an example of guaranteed and dual guaranteed Voronoi diagrams.

Guaranteed and dual guaranteed Voronoi cells are important as they yield approximations of the ith Voronoi cell and its centroid under uncertainties. In particular, if we know $gV_i(\mathbb{D})$ and $dgV_i(\mathbb{D})$ one can find an approximation to $\mathbf{c}_{V_i}(t)$ with a known bounded error using the following proposition from [30, Proposition 5.2].

Proposition 1: Let U, V, W be three sets such that $U \subseteq V \subseteq W$. Then, for any density function ϕ the following holds

$$\|\mathbf{c}_V - \mathbf{c}_U\| \leq \mathrm{dm}(W)\left(1 - \frac{m_U}{m_W}\right).$$

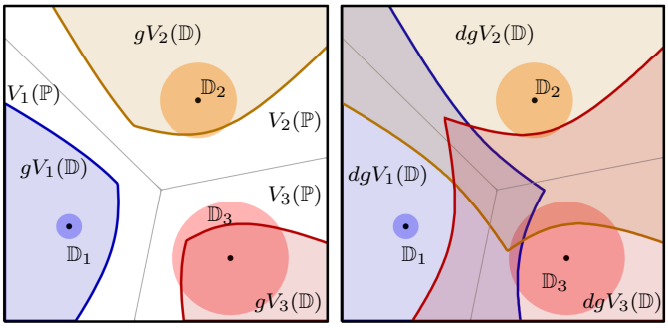

Fig. 1: A guaranteed Voronoi Diagram (left) and a dual guaranteed Voronoi Diagram (right). The true location of the agents $\mathbb{P} = \{\mathbf{p}_1, \mathbf{p}_2, \mathbf{p}_3\}$ is marked by the black dots, while the regions of uncertainties are denoted by the circular regions $\mathbb{D}_i$.

In brief, Proposition 1 implies that $\|\mathbf{c}_{V_i} - \mathbf{c}_{gV_i}\| \leq \mathrm{dm}(dgV_i)(1 - m_{gV_i}/m_{dgV_i})$, where the arguments have been omitted for convenience and where all variables are known except for $\mathbf{c}_{V_i}$.

III. Problem Formulation

We are interested in finding a (locally) optimal deployment solution for the static coverage control problem for mobile sensor networks with restricted inter-agent sensing (or communication) capabilities. In particular, we assume that the agents can sense (or request) the position of their Voronoi neighbors at discrete, positive intervals of times and that the agents have incentives to reduce the sensing (or communication) rate of position information. That is, we want to reduce power consumption (or reduce communication bandwidth) by decreasing the frequency at which position information about other agents is sensed (or transmitted).

Accordingly, we denote the sequence of sensing times for the ith sensor as $\{t_k^i\}_{k \in \mathbb{Z}_{\geq 0}}$, where t_k^i marks the time instants at which the ith agent senses or receives position information from its neighbors. Without loss of generality we assume that $t_0^i = 0$, $\forall\ i \in \mathbb{N}$. Similarly, we define the time intervals between sensing instants as $\tau_k^i := t_{k+1}^i - t_k^i \geq \tau_{\min}$, where $\tau_{\min} > 0$ is the minimal allowable inter-execution interval [25]. Note that $\tau_{\min}$ represents a constraint on the sampling (or communication) frequency due to hardware and computational limitations. Overall, the sensing (or communication) among agents can be asynchronous, i.e., their sensing instants might not necessarily be the same $t_k^i \not\equiv t_k^j, \tau_k^i \not\equiv \tau_k^j\ \forall\ k \in \mathbb{Z}_{\geq 0}, i, j \in \mathbb{N}, i \neq j$.

In the following, we consider agents with single integrator dynamics (1) and radially bounded control inputs, i.e., $\mathbf{u}_i(t) \in \mathcal{B}[\mathbf{0}, v]$, $\forall\ t \geq 0$, where $v > 0$ represents their maximum velocity. Given that the control inputs are saturated, the same convergence properties of the continuous-time unsaturated Lloyd's algorithm may not hold [8]. Furthermore, we assume that the agents have knowledge of $\phi(\mathbf{q})$ for all $\mathbf{q} \in \mathbb{Q}$.

Having established the sensor's dynamics and sensing assumptions, we can state the main control objective as follows. Given a task domain $\mathbb{Q}$, density function $\phi(\mathbf{q})$, maximum

admissible velocity v, and minimum sensing interval $\tau_{\min}$, develop distributed, bounded motion control strategies for a group of agents such that the mobile sensor network achieves a configuration that locally minimizes the locational cost (2) and that increases the inter-execution sensing intervals τ_k^i $\forall\, i \in \mathbb{N}, k \in \mathbb{Z}_{\geq 0}$ (i.e., a reduction of the frequency at which other agents' position information is updated).

IV. Self-triggered Coverage Control

To achieve our control objective, we propose the following piecewise continuous, self-triggered saturated control version of Lloyds's method

$$\mathbf{u}_i(t) = \kappa \cdot \mathrm{sat}_{\frac{v}{\kappa}}(\mathbf{c}_{V_i}(t_k^i) - \mathbf{p}_i(t)), \quad \forall\, t \in [t_k^i, t_{k+1}^i) \tag{5}$$

where the selection of the discrete instants of communication $\{t_k^i\}_{k\in\mathbb{Z}_{\geq 0}}$ is discussed later in Section IV-B and the saturation function is defined as

$$\mathrm{sat}_a(\mathbf{x}) = \begin{cases} \mathbf{x}, & \text{if } \|\mathbf{x}\| \leq a \\ a\dfrac{\mathbf{x}}{\|\mathbf{x}\|}, & \text{otherwise} \end{cases}$$

for any $\mathbf{x} \in \mathbb{R}^n$ and some $a > 0$. Note that the control law satisfies the input constraints, i.e., $\mathbf{u}_i(t) \in \mathcal{B}[\mathbf{0}, v]$. According to Section III, we assume the ith agent is able to sense or receive current position information of its Voronoi neighbors at $t = t_k^i$. Therefore, the ith agent can accurately update its Voronoi cell, $V_i(\mathbb{P}(t_k^i))$, and centroid, $\mathbf{c}_{V_i}(t_k^i)$, at time t_k^i. Between sensing intervals, the centroid value in (5) is kept constant since the agent does not know its exact Voronoi region. Ideally, one would like to sample the position of the Voronoi neighbors fast enough such that the error between the data-sampled hold centroid and the true centroid remains small at all times. That is, we would like to design the inter-execution intervals $\{\tau_k^i\}_{k\in\mathbb{Z}_{\geq 0}}$ such that $\left\|\mathbf{c}_{V_i}(t_k^i) - \mathbf{c}_{V_i}(t)\right\| \leq \delta\ \forall\ t \in [t_k^i, t_k^i + \tau_k^i], k \in \mathbb{Z}_{\geq 0}$, where $\delta > 0$ is a tolerance control design parameter. To bound the difference between both quantities, one can compute the guaranteed and dual guaranteed Voronoi cells.

A. Guaranteed and Dual Guaranteed Voronoi Regions

Since the agents' velocities (and control inputs) are bounded by v at all times, the uncertainty regions in the position between sampling instants can be approximated as

$$\mathbb{X}_{ij}(\mathbf{p}_j(t_k^i), t_k^i, t) = \mathcal{B}[\mathbf{p}_j(t_k^i), (t - t_k^i)v] \quad \forall\, t \in [t_k^i, t_{k+1}^i)$$

for all $j \in \mathbb{N}_i(t_k^i)$, where $\mathbb{X}_{ij}(t) := \mathbb{X}_{ij}(\mathbf{p}_j(t_k^i), t_k^i, t)$ represents the uncertainty that the ith agent has about the jth sensor location as a function of time. Then, the ith agent guaranteed and dual guaranteed Voronoi cells can be computed as

$$gV_i(\mathbb{X}_i(t)) := \{\mathbf{q} \in \mathbb{Q} \mid \|\mathbf{p}_i(t) - \mathbf{q}\| \leq \min_{\mathbf{y}\in\mathbb{X}_{ij}(t)} \|\mathbf{y} - \mathbf{q}\|\},$$

$$dgV_i(\mathbb{X}_i(t)) := \{\mathbf{q} \in \mathbb{Q} \mid \|\mathbf{p}_i(t) - \mathbf{q}\| \leq \max_{\mathbf{y}\in\mathbb{X}_{ij}(t)} \|\mathbf{y} - \mathbf{q}\|\},$$

for all $j \in \mathbb{N}_i(t_k^i)$, where $\mathbb{X}_i(t) := \{\mathbf{p}_i(t), \{\mathbb{X}_{ij}(t)\}_{j\in\mathbb{N}_i(t_k^i)}\}$ represents the collection of location uncertainty regions for the ith agent. In [30, Lemma 4.1] it is shown that for a group of agents with same maximum velocity, the set of neighbors

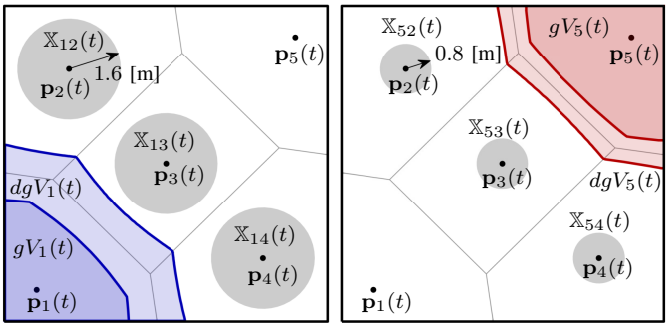

Fig. 2: Example of guaranteed and dual guaranteed Voronoi cells for two agents with same set of Voronoi neighbors at a given time t, $\mathbb{N}_1(t) = \mathbb{N}_5(t) = \{2, 3, 4\}$, but with different sampling instants and, therefore, different regions of position uncertainties. The regions of uncertainties for the first agent (see left figure) are given by $\mathbb{X}_{1j}(t) = \mathcal{B}[\mathbf{p}_j(t_k^1), 1.6]$. The regions of uncertainties for the fifth agent (see right figure) at the same time are given by $\mathbb{X}_{5j}(t) = \mathcal{B}[\mathbf{p}_j(t_k^5), 0.8]$. The regular Voronoi cells (delimited by the fine black lines) for the first agent and fifth agent have equal size. However, their guaranteed and dual guaranteed Voronoi cells differ in size and shape.

at $t = t_k^i$, i.e., $\mathbb{N}_i(t_k^i)$, is enough to describe the evolution of $gV_i(\mathbb{X}_i(t))\ \forall\ t \in [t_k^i, t_{k+1}^i)$. That is, no new neighbor can appear within sampling instants and affect the guaranteed Voronoi cell. Similarly, one has that adding information of new neighbors can only decrease the size of $dgV_i(\mathbb{X}_i(t))$ [30, Lemma 4.3]. Both properties will be used later in Section IV-C. Note that the uncertainty region about a particular jth sensor at any given time can differ among its neighbors, that is, $\mathbb{X}_{ij}(t) \not\equiv \mathbb{X}_{\ell j}(t)$ for $i, \ell \in \mathbb{N}_j(t),\ i \neq \ell$ (see Fig. 2). Similarly, note that by definition $gV_i(\mathbb{X}_i(t)) = V_i(\mathbb{P}(t)) = dgV_i(\mathbb{X}_i(t))$ for $t = t_k^i$. Furthermore, we can also establish the following relationships among Voronoi regions within the inter-execution sensing intervals.

Proposition 2: Let $\|\dot{\mathbf{p}}_i(t)\| \leq v\ \forall\ t \geq 0,\ \forall\ i \in \mathbb{N}$. Then,

a) $gV_i(\mathbb{X}_i(t_k^i + \tau)) \subseteq V_i(\mathbb{P}(t_k^i + \tau))$;
b) $dgV_i(\mathbb{X}_i(t_k^i + \tau)) \supseteq V_i(\mathbb{P}(t_k^i + \tau))$;
c) $gV_i(\mathbb{X}_i(t_k^i + \tau)) \subseteq V_i(\mathbb{P}(t_k^i))$;
d) $dgV_i(\mathbb{X}_i(t_k^i + \tau)) \supseteq V_i(\mathbb{P}(t_k^i))$

$\forall\ \tau \in [0, \tau_k^i)$.

Proof: The first two statements follow from the definition of guaranteed and dual guaranteed Voronoi cells. To prove the third statement it suffices to show that for any $\mathbf{x} \in \mathbb{Q}$, $\mathbf{x} \in gV_i(\mathbb{X}_i(t_k^i + \tau))$ implies $\mathbf{x} \in gV_i(\mathbb{P}(t_k^i))$. Accordingly, assume that $\|\dot{\mathbf{p}}_i(t)\| \leq v$ and that $\mathbf{x} \in gV_i(\mathbb{X}_i(t_k^i + \tau))$. Then, $\forall\ j \in \mathbb{N}_i(t_k^i)$, we have that

$$\|\mathbf{x} - \mathbf{p}_i(t_k + \tau)\| \leq \min_{\mathbf{y}\in\mathbb{X}_{ij}(t_k^i+\tau)} \|\mathbf{x} - \mathbf{y}\|$$

$$\left\|\mathbf{x} - \mathbf{p}_i(t_k^i)\right\| - v\tau \leq \left\|\mathbf{x} - \mathbf{p}_i(t_k^i + \tau)\right\| \leq \left\|\mathbf{x} - \mathbf{p}_j(t_k^i)\right\| - v\tau$$

$$\left\|\mathbf{x} - \mathbf{p}_i(t_k^i)\right\| \leq \left\|\mathbf{x} - \mathbf{p}_j(t_k^i)\right\|$$

which implies that $\mathbf{x} \in V_i(\mathbb{P}(t_k^i))$. To prove the fourth statement one can use similar arguments. We would like to show that $\mathbf{x} \in V_i(\mathbb{X}_i(t_k^i))$ implies that $\left\|\mathbf{x} - \mathbf{p}_i(t_k^i + \tau)\right\| \leq$

$\max_{\mathbf{y}\in\mathbb{X}_{ij}(t_k^i+\tau)} \|\mathbf{x}-\mathbf{y}\| \leq \left\|\mathbf{x}-\mathbf{p}_j(t_k^i)\right\| + v\tau$ for all $j \in \mathbb{N}_i(t_k^i)$. Accordingly, assume that $\mathbf{x} \in V_i(\mathbb{X}_i(t_k^i))$. Then,

$$\begin{aligned}\left\|\mathbf{x}-\mathbf{p}_i(t_k^i)\right\| &\leq \left\|\mathbf{x}-\mathbf{p}_j(t_k^i)\right\| \\ \left\|\mathbf{x}-\mathbf{p}_i(t_k^i)+\mathbf{p}_i(t_k^i+\tau)-\mathbf{p}_i(t_k^i+\tau)\right\| &\leq \left\|\mathbf{x}-\mathbf{p}_j(t_k^i)\right\| \\ \left\|\mathbf{x}-\mathbf{p}_i(t_k^i+\tau)\right\| - v\tau &\leq \left\|\mathbf{x}-\mathbf{p}_j(t_k^i)\right\| \\ \left\|\mathbf{x}-\mathbf{p}_i(t_k^i+\tau)\right\| &\leq \left\|\mathbf{x}-\mathbf{p}_j(t_k^i)\right\| + v\tau\end{aligned}$$

which completes the proof. ∎

In what follows, we will omit the set arguments when defining Voronoi cells to reduce cluttering of equations and use time as argument to imply that the regions change over time. That is, we will opt for $V_i(t)$, $gV_i(t)$, and $gdV_i(t)$ in lieu of $V_i(\mathbb{P}(t))$, $gV_i(\mathbb{X}_i(t))$, and $dgV_i(\mathbb{X}_i(t))$ unless deemed necessary.

B. Inter-execution Intervals

Having defined the control law (5) and formulated the agents' guaranteed and dual guaranteed Voronoi cells between sensing instants, we can proceed to establish the self-triggering rule for the inter-execution intervals $\{\tau_k^i\}_{k\in\mathbb{Z}_{\geq 0}}$.

Let us define the set of allowable inter-execution intervals as $\mathbb{T} \in [\tau_{\min}, \tau_{\max}]$, where $\tau_{\max} > \tau_{\min}$ is the maximal allowable interval for robustness purposes [35]. As aforementioned, we would like to design $\{\tau_k^i\}_{k\in\mathbb{Z}_{\geq 0}}$ such that $\left\|\mathbf{c}_{V_i}(t_k^i) - \mathbf{c}_{V_i}(t_k^i+\tau)\right\|$ is bounded by some constant design parameter $\delta > 0 \ \forall \ \tau \in [0, \tau_k^i]$. Therefore, consider the following inequality

$$\begin{aligned}&\left\|\mathbf{c}_{V_i}(t_k^i) - \mathbf{c}_{V_i}(t_k^i+\tau)\right\| \\ &= \left\|\mathbf{c}_{V_i}(t_k^i) - \mathbf{c}_{gV_i}(t_k^i+\tau) - \mathbf{c}_{V_i}(t_k^i+\tau) + \mathbf{c}_{gV_i}(t_k^i+\tau)\right\| \\ &\leq \left\|\mathbf{c}_{V_i}(t_k^i) - \mathbf{c}_{gV_i}(t_k^i+\tau)\right\| + \left\|\mathbf{c}_{V_i}(t_k^i+\tau) - \mathbf{c}_{gV_i}(t_k^i+\tau)\right\|.\end{aligned}$$

Using Propositions 1 and 2 yields that

$$\begin{aligned}&\left\|\mathbf{c}_{V_i}(t_k^i) - \mathbf{c}_{V_i}(t_k^i+\tau)\right\| \\ &\qquad \leq 2\mathrm{dm}(dgV_i(t_k^i+\tau))\left(1 - \frac{m_{gV_i}(t_k^i+\tau)}{m_{dgV_i}(t_k^i+\tau)}\right). \quad (6)\end{aligned}$$

Hence, to guarantee that $\left\|\mathbf{c}_{V_i}(t_k^i) - \mathbf{c}_{V_i}(t_k^i+\tau)\right\| \leq \delta, \forall\ \tau \leq \tau_k^i$, it suffices to enforce that

$$\mathrm{dm}(dgV_i(t_k^i+\tau))\left(1 - \frac{m_{gV_i}(t_k^i+\tau)}{m_{dgV_i}(t_k^i+\tau)}\right) \leq \frac{\delta}{2}. \quad (7)$$

In addition, one would like to guarantee that the agents do not come arbitrarily close from each other, i.e., $\mathbf{p}_i(t) \not\to \mathbf{p}_j(t)$ for $i \neq j$, in order to prevent degenerate Voronoi diagrams. Given that the agents do not know the location of their neighbors or where these are heading between sensing intervals, we cannot guarantee that they will remain sufficiently apart. One approach to enforce that agents remain distant from each others is to guarantee that each agent's data-sampled centroid remains within the agent's guaranteed Voronoi cell, i.e., $\mathbf{c}_{V_i}(t_k^i) \in gV_i(t_k^i+\tau)$. If we define $\rho_{gV_i}(t+\tau)$ as the shortest distance between $\mathbf{c}_{gV_i}(t+\tau)$ and $\partial gV_i(t+\tau)$, then it suffices to require that $\mathbf{c}_{V_i}(t_k^i) \in \mathcal{B}[\mathbf{c}_{gV_i}(t_k^i+\tau), \rho_{gV_i}(t_k^i+\tau)]$ or, equivalently, that

$$\left\|\mathbf{c}_{V_i}(t_k^i) - \mathbf{c}_{gV_i}(t_k^i+\tau)\right\| \leq \rho_{gV_i}(t_k^i+\tau).$$

Algorithm 1: Self-triggered Coverage Control Law

```
/* Code for each Agent, i ∈ ℕ                    */
Data: φ(q), ℚ, p_i, τ_min, τ_max, δ, v, κ
Result: u_i
t ← 0, t_0^i ← 0, k ← 0;
while t ≤ Final Time do
    Update p_i;
    if t ≥ t_k^i then
        Detect neighbors, ℕ_j;
        Update p_j ∀ j ∈ ℕ_j;
        Compute V_i, c_{V_i};
        τ_k^i ← τ_min;
        for ℓ ← 2 to τ_max/τ_min do
            τ ← ℓτ_min;
            Estimate Uncertainty 𝕏_i(t_k^i + τ);
            Compute gV_i(t_k^i + τ), dgV_i(t_k^i + τ);
            Compute m_{gV_i}, m_{dgV_i}, ρ_{gV_i};
            Compute h(t_k^i + τ);
            if h(t_k^i + τ) > 0 then
                Break for-loop;
            else
                τ_k^i ← τ;
            end
        end
        t_{k+1}^i ← t_k^i + τ_k^i;
        k ← k + 1;
    end
    u_i(t) ← κ · sat_{v/κ}(c_{V_i} − p_i);
    Update t;
end
```

Using once again Proposition 1 and combining the above inequality with (7), the objective reduces to enforcing the following condition

$$\begin{aligned}&\mathrm{dm}(dgV_i(t_k^i+\tau))\left(1 - \frac{m_{gV_i}(t_k^i+\tau)}{m_{dgV_i}(t_k^i+\tau)}\right) \\ &\qquad \leq \min\left(\rho_{gV_i}(t_k^i+\tau), \frac{\delta}{2}\right), \ \forall \tau \in [0, \tau_k^i].\end{aligned}$$

Therefore, we propose to update the inter-execution intervals according to

$$\tau_k^i = \max_{\tau}\{\tau \in \mathbb{T} \mid h(s) \leq 0, \ \forall\ s \in [0,\tau]\} \quad (8a)$$

$$\begin{aligned}h(s) =& \mathrm{dm}(dgV_i(t_k^i+s))\left(1 - \frac{m_{gV_i}(t_k^i+s)}{m_{dgV_i}(t_k^i+s)}\right) \\ &- \min\left(\rho_{gV_i}(t_k^i+s), \frac{\delta}{2}\right). \quad (8b)\end{aligned}$$

The synthesis of the distributed, data-sampled, piece-wise continuous control law (5) and the inter-execution sensing interval condition (8) can be formalized by Algorithm 1. Note that in illustrating the algorithm we assumed that $\mathbb{T}$ is discrete, i.e., that each element is a multiple of $\tau_{\min}$.

Remark 2: The set of allowable inter-execution intervals $\mathbb{T}$ can be continuous or discrete (e.g., $\mathbb{T} = \{\tau_1, \cdots, \tau_m\}$, where $\tau_\ell > \tau_{\ell-1}, \tau_1 = \tau_{\min}, \tau_m = \tau_{\max}$). In general, the

discretization of $\mathbb{T}$ leads to less computations by reducing the times at which the self-triggering condition is evaluated at the expense of slightly shorter sampling intervals. For purposes of implementation, the simulations and experimental results in Sections V and VI will assume a discrete interval given by multiples of $\tau_{\min}$, i.e., $\mathbb{T} = \{\tau_{\min}, 2\tau_{\min}, 3\tau_{\min}, \cdots, \tau_{\max}\}$, where $\tau_{\max}$ is also a multiple of $\tau_{\min}$.

In Section IV-C we will show that execution of Algorithm 1 guarantees that the locational cost function is monotonically decreasing outside of a bounded neighborhood of a CVT and that the configuration $\mathbb{P}(t)$ converges to a CVT once the data-sampled centroid errors converge to zero. But first, we will show that (8) has always a positive solution. That is, $\exists \tau^\star > 0$ such that the solutions of (8) are always lower bounded by $\tau^\star$, which in turn implies that the proposed triggering condition does not produce unwanted Zeno behavior. We start by introducing the following Lemma from [39, Lemma 3.2] and, then, proceed with the statement on the lower bound of τ_k^i.

Lemma 1: Let $S \subset \mathbb{Q}$ be a convex set with finite mass $m_S > 0$ and volume $\mathcal{V}_S$. Define $\mathcal{V}_\mathbb{Q}$ as the volume of $\mathbb{Q}$. Then, for any $\sigma \geq 0$, it holds that

$$\rho_S \geq \delta_\sigma = \frac{\eta_\sigma^2}{64\ \mathrm{dm}(S)^{2n-1}}$$

where ρ_S is the shortest distance from $\mathbf{c}_S$ to ∂S and $\eta_\sigma := \sup_{\eta \in E_\sigma} \eta$ for $E_\sigma = \{\eta \in [0, \mathcal{V}_\mathbb{Q}] \mid m_S \leq \sigma, \mathcal{V}_S \leq \eta\}$.

The above lemma implies that for any convex set S of non-zero volume, the distance ρ_S can be lower bounded by a positive constant. We now state the following assumption.

Assumption 1: $\exists \epsilon > 0$ such that $\left\|\mathbf{p}_i(t_k^i) - \mathbf{p}_j(t_k^i)\right\| \geq \epsilon$ and $\left\|\mathbf{p}_i(t_k^i) - \mathbf{q}\right\| \geq \frac{\epsilon}{2}$ for all $i \in \mathbb{N}, i \neq j, k \in \mathbb{Z}_{\geq 0}$ and $\mathbf{q} \in \partial\mathbb{Q}$.

Assumption 1 implies that the ith agent's Voronoi cell contains an n-ball $\mathcal{B}[\mathbf{p}_i(t_k^i), \frac{\epsilon}{2}]$ at each sampling time or, equivalently, that the volume of the ith Voronoi cell can be lower bounded by the volume of such ball, i.e., $\mathcal{V}_n(\frac{\epsilon}{2})$. Given that the velocities of the agents are bounded by v, it also means that the volume of the guaranteed Voronoi cells can be lower bounded by $\mathcal{V}_n(\frac{\epsilon - 2v\tau}{2})$. This assumption can be seen as a result of Lloyd's algorithm which tends to sparsely distribute the agent across the task domain. It is also important to mention that similar assumptions on the Voronoi cell properties have been proposed in previous work. For example, in [28] it is assumed that the velocities of the centroids are bounded, which in general cannot be guaranteed.

Proposition 3: Suppose that $\|\dot{\mathbf{p}}_i(t)\| \leq v\ \forall\ t \geq 0$ and that Assumption 1 holds for some $\epsilon > 0$. Then, $\exists \tau^\star > 0$ such that $h(s) \leq 0\ \forall\ s \in [0, \tau^\star]$, i.e., $\tau_k^i \geq \tau^\star\ \forall\ k \in \mathbb{Z}_{\geq 0}$.

Proof: To prove the above statement, we will use the following upper bound function of (8b)

$$\bar{h}(s) = \mathrm{dm}(\mathbb{Q}) \left(1 - \frac{m_{gV_i}(t_k^i + s)}{m_{dgV_i}(t_k^i + s)}\right) - \frac{\rho_{gV_i}(t_k^i + s)\delta}{2\rho_{gV_i}(t_k^i + s) + \delta} \tag{9}$$

where the second term is a continuous differentiable lower bound approximation of the minimum function [40] for $\delta \geq 0$ and $\rho_{gV_i}(t_k^i + s) \geq 0$. Since $h(s) \leq \bar{h}(s)\ \forall\ s \geq 0$, it suffices to show that $\exists \tau^\star > 0$ such that $\bar{h}(s) \leq 0\ \forall\ s \in [0, \tau^\star]$.

Assume that $\|\dot{\mathbf{p}}_i(t)\| \leq v$ and $\left\|\mathbf{p}_i(t_k^i) - \mathbf{p}_j(t_k^i)\right\| \geq \epsilon$ for some $\epsilon > 0$ and $\forall\ j \in \mathbb{N}_i(t_k^i)$. Pick $\tau \in (0, \epsilon/2v)$. The latter implies that

$$\begin{aligned}\left\|\mathbf{p}_i(t_k^i + \tau) - \mathbf{p}_j(t_k^i + \tau)\right\| &\geq \left\|\mathbf{p}_i(t_k^i) - \mathbf{p}_j(t_k^i)\right\| - 2v\tau \\ &> \epsilon - 2v\tau > 0\end{aligned}$$

which means that $gV_i(t_k^i + \tau) \neq \emptyset$ and, therefore, $\rho_{gV_i}(t_k^i + s) \geq \delta_\epsilon \in (0, \mathrm{dm}(V_i(t_k^i))$ for all $s \in [0, \tau]$ and for some $\delta_\epsilon > 0$, where we used Lemma 1 and Proposition 2. By evaluating (9) for $s = 0$ one obtains that

$$\bar{h}(0) = -\frac{\rho_{gV_i}(t_k^i)\delta}{2\rho_{gV_i}(t_k^i) + \delta} \leq -\frac{\delta_\epsilon \delta}{\mathrm{dm}(\mathbb{Q}) + \delta} < 0$$

where we used the fact that $\rho_{gV_i}(t_k^i) \leq \mathrm{dm}(\mathbb{Q})/2$.

Now, since $\mathbf{c}_{gV_i}$ and the points in the boundary $\mathbf{q} \in \partial gV_i$ are smooth continuous functions of $\mathbf{p}_i(t)$ and $\mathbf{p}_j(t)$ (the latter from smoothness of $\phi(\mathbf{q})$), one has that $\rho_{gV_i}(t_k^i + s)$ is also smooth in the interval $s \in [0, \tau)$, which implies that $\exists \delta_\rho > 0$ such that $\left\|d\rho_{gV_i}(t_k^i + s)/ds\right\| \leq \delta_\rho$. Next, consider the derivative of $\bar{h}(\tau)$

$$\begin{aligned}\frac{d\bar{h}(\tau)}{d\tau} =& \mathrm{dm}(\mathbb{Q}) \frac{\dot{m}_{dgV_i}(t_k^i + \tau) m_{gV_i}(t_k^i + \tau)}{m_{dgV_i}^2(t_k^i + \tau)} \\ &- \mathrm{dm}(\mathbb{Q}) \frac{\dot{m}_{gV_i}(t_k^i + \tau) m_{dgV_i}(t_k^i + \tau)}{m_{dgV_i}^2(t_k^i + \tau)} \\ &- \frac{\dot{\rho}_{gV_i}(t_k^i + \tau)\delta^2}{(2\rho_{gV_i}(t_k^i + \tau) + \delta)^2}.\end{aligned}$$

Taking the norm of the above equation yields

$$\begin{aligned}\left\|\frac{d\bar{h}(\tau)}{d\tau}\right\| \leq& \mathrm{dm}(\mathbb{Q}) \frac{\|\dot{m}_{dgV_i}(t)\|\, m_{gV_i}(t) + \|\dot{m}_{gV_i}(t)\|\, m_{dgV_i}(t)}{m_{dgV_i}^2(t)} \\ &+ \frac{\delta^2 \delta_\rho}{(2\delta_\epsilon + \delta)^2}\end{aligned}$$

where $t = t_k^i + \tau$ for short of notation. Then, applying Lemma 2 from Appendix A and the fact that $\exists\ m_\epsilon > 0$ such that $m_{dgV_i}(t) \geq m_{V_i}(t_k^i) \geq m_\epsilon$ (from Proposition 2 and the positiveness of $\phi(\mathbf{q})$) one obtains that

$$\begin{aligned}\left\|\frac{d\bar{h}(\tau)}{d\tau}\right\| \leq& \mathrm{dm}(\mathbb{Q}) \frac{\|\dot{m}_{dgV_i}(t)\| + \|\dot{m}_{gV_i}(t)\|}{m_{V_i}(t)} + \frac{\delta^2 \delta_\rho}{(2\delta_\epsilon + \delta)^2} \\ \leq& \frac{v\phi_{\max}\mathrm{dm}(\mathbb{Q})^2}{\epsilon - 2v\tau} \mathcal{A}_n\left(\frac{1}{2}\mathrm{dm}(\mathbb{Q})\right) \frac{2 + |\mathbb{N}_i(t_k^i)|}{m_\epsilon} \\ &+ \frac{\delta^2 \delta_\rho}{(2\delta_\epsilon + \delta)^2} \\ :=& L_\epsilon\end{aligned}$$

which is finite since $\epsilon > 2v\tau$. This implies that the derivative of $\bar{h}(s)$ is bounded by some constant $L_\epsilon < \infty$ for all $s \in [0, \tau)$, where the constant can be completely described by the initial position of the ith agent at time t_k^i relative to its Voronoi neighbors. Note that in addition, the number of Voronoi neighbors $|\mathbb{N}_i(t_k^i)|$ is equal or less than $N - 1$ and it approaches six on average when $n = 2$.

Now, define

$$a := v\phi_{\max}\mathrm{dm}(\mathbb{Q})^2\mathcal{A}_n\left(\frac{1}{2}\mathrm{dm}(\mathbb{Q})\right)\frac{1+N}{m_\epsilon},$$
$$b := \frac{\delta^2\delta_\rho}{(2\delta_\epsilon+\delta)^2},$$
$$c := \frac{\delta_\epsilon\delta}{\mathrm{dm}(\mathbb{Q})+\delta}.$$

Let $\tau^\star$ mark the first time that $\bar{h}(\cdot)$ crosses zero, i.e., $\bar{h}(\tau^\star) = 0$. Applying the Mean Value Theorem and noting that $L_\epsilon \leq \frac{a}{\epsilon-2v\tau} + b$ we have that

$$c = \left\|\bar{h}(\tau^\star) - \bar{h}(0)\right\| \leq L_\epsilon\tau^\star \leq \frac{a\tau^\star}{\epsilon-2v\tau^\star} + b\tau^\star. \quad (10)$$

Solving for $\tau^\star$ we get that the two solutions $\tau^\star_{1,2}$ to the above inequality

$$\tau^\star_{1,2} = \frac{a+2vc+b\epsilon \pm \sqrt{(a+2vc+b\epsilon)^2 - 8vbc\epsilon}}{4bv}$$
$$= \frac{a+2vc+b\epsilon \pm \sqrt{a^2+2ab\epsilon+4vac+(2vc-b\epsilon)^2}}{4bv}$$

are positive. Picking the smallest of the two solutions we can conclude that $h(s) \leq \bar{h}(s) \leq 0 \ \forall\ s \in [0, \tau^\star]$, where

$$\tau^\star = \frac{a+2vc+b\epsilon - \sqrt{(a+2vc+b\epsilon)^2 - 8vbc\epsilon}}{4bv} > 0 \quad (11)$$

which is positive for all $\epsilon > 0$. ∎

Proposition 3 states that, if the ith agent does not start at the same position of another agent, the solution τ^i_k is always positive. Moreover, the solutions to (8) can always be lower bounded by some positive $\tau^\star$ if a minimum distance ϵ among agents can be guaranteed at all sampling times t^i_k. The latter would imply that the self-triggered control does not exhibit Zeno behavior and can be digitally implemented.

In practice, we do not only want $\tau^\star$ to be positive, but to be equal or greater than some given $\tau_{\min}$. However, the lower bound $\tau^\star$ computed in (11) is a function of ϵ. Although we cannot guaranteed that a minimum distance ϵ can be enforced at all sampling times among agents, it is well known that Lloyd's descent algorithm tends to gradually distribute agents more sparsely across the space based on the density function. In addition, note that the self-triggering rule (8) guarantees that the agents always remain within their own guaranteed Voronoi cells between sampling intervals.

Next, we provide an explicit lower bound on sensing intervals as a function of ϵ, v, and δ that satisfies the constraint $\tau^i_k \geq \tau_{\min}\ \forall\ k$.

Corollary 1: Suppose that Assumption 1 holds for some $\epsilon > 0$. Let $\tau' \in (0, \frac{\epsilon}{2v})$ and pick

$$\delta \leq \frac{\phi^2_{\min}\pi^n(\epsilon-2v\tau')}{2^{2n+9}\phi^2_{\max}\Gamma\left(\frac{n}{2}+1\right)^2} \quad (12)$$

where $\Gamma : \mathbb{Z}_{\geq 0} \to \mathbb{R}_{\geq 0}$ is the Euler's gamma function. Then,

$$\tau^\star \geq \min\left\{\frac{\delta\epsilon\mathcal{V}_n(\epsilon/2)}{2v\left(\beta+\delta\mathcal{V}_n(\epsilon/2)\right)}, \tau'\right\} \quad (13)$$

where

$$\beta := \phi^{-1}_{\min}\phi_{\max}\mathrm{dm}(\mathbb{Q})^2\mathcal{A}_n\left(\frac{1}{2}\mathrm{dm}(\mathbb{Q})\right)(1+N).$$

Moreover, if Assumption 1 holds for

$$\epsilon > 2\max\left\{\left(\frac{\tau_{\min}v}{\delta\pi^{\frac{n}{2}}}\Gamma\left(\frac{n}{2}+1\right)\beta + v\tau_{\min}\mathcal{V}_n(\mathrm{dm}(\mathbb{Q})/2)\right)^{\frac{1}{n+1}}, v\tau_{\min}\right\} \quad (14)$$

then, $\tau^\star \geq \tau_{\min}$.

Proof: Suppose Assumption 1 holds and pick δ according to (12). Invoking Lemma 1 yields

$$\rho_{gV_i}(t^i_k+\tau) \geq \left(\frac{\phi_{\min}\mathcal{V}_n(\frac{\epsilon-2v\tau}{2})}{4\phi_{\max}}\right)^2\frac{1}{64(\epsilon-2v\tau)^{2n-1}}$$
$$= \frac{\phi^2_{\min}\pi^n(\epsilon-2v\tau)^{2n}}{2^{2n}2^4\phi^2_{\max}\Gamma(\frac{n}{2}+1)^2}\frac{1}{2^6(\epsilon-2v\tau)^{2n-1}}$$
$$\geq \frac{\delta}{2}$$

$\forall\tau \in [0, \tau']$, where we used the fact that $\mathcal{V}_n(r) = \pi^{n/2}\Gamma(\frac{n}{2}+1)^{-1}r^n$ for any n-ball of radius r. Then, (8b) can be upper bounded by

$$\bar{h}(\tau) = \mathrm{dm}(\mathbb{Q})\left(1 - \frac{m_{gV_i}(t^i_k+\tau)}{m_{dgV_i}(t^i_k+\tau)}\right) - \frac{\delta}{2}, \quad \forall\tau \in [0, \tau'].$$

Revisiting the proof of Proposition 3, one can show that $b = 0$ and that (10) reduces to

$$\frac{\delta}{2} = \left\|\bar{h}(\tau^\star) - \bar{h}(0)\right\| \leq L_\epsilon\tau^\star \leq \frac{a\tau^\star}{\epsilon-2v\tau^\star}$$
$$\delta(\epsilon-2v\tau^\star) \leq 2v\phi_{\max}\mathrm{dm}(\mathbb{Q})^2\mathcal{A}_n\left(\frac{1}{2}\mathrm{dm}(\mathbb{Q})\right)\frac{1+N}{m_\epsilon}\tau^\star$$

for $\tau^\star \in [0, \tau']$. Noting that $m_\epsilon \geq \mathcal{V}_n\left(\frac{\epsilon}{2}\right)\phi_{\min}$, we then have that

$$\delta\epsilon\mathcal{V}_n(\epsilon/2) \leq 2v\beta\tau^\star + 2\delta v\mathcal{V}_n(\epsilon/2)\tau^\star$$

and solving for $\tau^\star$ yields

$$\tau^\star \geq \frac{\delta\epsilon\mathcal{V}_n(\epsilon/2)}{2v\left(\beta+\delta\mathcal{V}_n(\epsilon/2)\right)}.$$

Note that the above analysis might not be valid if $\tau^\star > \tau'$. Therefore, it suffices to take the minimum function as in (13), which completes the proof for the first statement.

Now, consider the second statement. Since $\epsilon \geq 2v\tau_{\min}$, we can pick $\tau' \geq \tau_{\min}$. Then, to prove that $\tau^\star \geq \tau_{\min}$, it is enough to show that the first argument of (13) is equal or greater than $\tau_{\min}$. Taking into account that $\mathcal{V}_n(\epsilon/2) \leq \mathcal{V}_n(\mathrm{dm}(\mathbb{Q})/2)$, since $\epsilon \leq \mathrm{dm}(\mathbb{Q})$, one has that (13) can be bounded by

$$\tau^\star \geq \frac{\delta\epsilon\mathcal{V}_n(\epsilon/2)}{2v\left(\beta+\delta\mathcal{V}_n(\mathrm{dm}(\mathbb{Q}/2))\right)}.$$

Then, using the formula for the volume yields

$$\tau^\star \geq \frac{\delta\pi^{\frac{n}{2}}\Gamma\left(\frac{n}{2}+1\right)^{-1}2^{-n}\epsilon^{n+1}}{2v\left(\beta+\delta\mathcal{V}_n(\mathrm{dm}(\mathbb{Q}/2))\right)}$$

and finally substituting for ϵ one obtains that $\tau^\star \geq \tau_{\min}$, which completes the proof. ∎

The above corollary provides a closed-form expression for a lower bound on the time interval assuming a minimum distance ϵ among agents is kept at all times. This lower bound is extremely conservative and tighter bounds can be computed if the number of Voronoi neighbors as well as the diameter of the Voronoi cells can be upper bounded. In addition, note that (14) provides a guideline of how to pick δ and v such that (8a) is always satisfied given $\tau_{\min}$ and ϵ. In particular, larger values of δ and smaller values of v lead to larger sampling intervals as well as the feasibility of (8) for all times. Note that feasibility of (8) also implies the existence of guaranteed Voronoi cells at all times.

C. Minimization of Locational Cost and Convergence to CVT

Herein, we will show that the locational cost function is monotonically decreasing outside of a bounded neighborhood of a CVT and that the multi-agent group asymptotically converges to a CVT if the error between the data-sampled centroids and the true centroids converges to zero.

Proposition 4: Consider a group of N mobile agents with dynamics and control inputs given by (1) and (5), respectively. Assume the update intervals $\tau_k^i \in [\tau_{\min}, \tau_{\max}]$ evolve according to (8), for some $\delta > 0$, and that Proposition 3 holds for some $\tau^\star \geq \tau_{\min}$. Then, for all $\mathbf{p}_i(t) \notin \mathcal{B}[\mathbf{c}_{V_i}(t), N\hat{\delta}(t)]$, where $\hat{\delta}(t) = \min\{\delta, \max_{i\in\mathbb{N}} \left\|\mathbf{c}_{V_i}(t) - \mathbf{c}_{V_i}(t_k^i)\right\|\} \leq \delta$, $\mathcal{H}(\mathbb{P}(t))$ is monotonically decreasing.

Proof: Consider the locational cost function in (2). Taking the partial derivative with respect to $\mathbf{p}_i$ we obtain

$$\begin{aligned}\frac{\partial \mathcal{H}(\mathbb{P}(t))}{\partial \mathbf{p}_i(t)} =& -\int_{V_i(\mathbb{P}(t))} (\mathbf{q}-\mathbf{p}_i(t))^T\phi(\mathbf{q})d\mathbf{q} \\ &+ \sum_{j\in\mathbb{N}_i(t)} \int_{\partial V_{ij}(\mathbb{P}(t))} \|\mathbf{q}-\mathbf{p}_i(t)\|^2 \frac{(\mathbf{q}-\mathbf{p}_i(t))^T}{\|\mathbf{p}_i(t)-\mathbf{p}_j(t)\|}\phi(\mathbf{q})d\mathbf{q} \\ &- \sum_{j\in\mathbb{N}_i(t)} \int_{\partial V_{ij}(\mathbb{P}(t))} \|\mathbf{q}-\mathbf{p}_j(t)\|^2 \frac{(\mathbf{q}-\mathbf{p}_i(t))^T}{\|\mathbf{p}_i(t)-\mathbf{p}_j(t)\|}\phi(\mathbf{q})d\mathbf{q} \\ =& -2\int_{V_i(\mathbb{P}(t))} (\mathbf{q}-\mathbf{p}_i(t))^T\phi(\mathbf{q})d\mathbf{q} = 2m_{V_i}(t)(\mathbf{p}_i(t)-\mathbf{c}_{V_i}(t))^T\end{aligned}$$

where we used Leibniz Integral Rule [36] and the fact that $||\mathbf{p}_i(t)-\mathbf{q}|| = ||\mathbf{p}_j(t)-\mathbf{q}||\ \forall\ \mathbf{q}\in\partial V_{ij}(t)$. Then, the time derivative of (2) can be computed as

$$\begin{aligned}\frac{d\mathcal{H}(\mathbb{P}(t))}{dt} =& \sum_{i=1}^N \frac{\partial \mathcal{H}(\mathbb{P}(t))}{\partial \mathbf{p}_i(t)}\cdot\dot{\mathbf{p}}_i(t) \\ =& \sum_{i=1}^N -2\kappa m_{V_i}(t)(\mathbf{p}_i(t)-\mathbf{c}_{V_i}(t))^T \mathrm{sat}_{\frac{v}{\kappa}}(\mathbf{p}_i(t)-\mathbf{c}_{V_i}(t_k^i)) \\ =& \sum_{i=1}^N -2\kappa m_{V_i}(t)(\mathbf{p}_i(t)-\mathbf{c}_{V_i}(t))^T \\ &\cdot \mathrm{sat}_{\frac{v}{\kappa}}(\mathbf{p}_i(t)-\mathbf{c}_{V_i}(t)+\mathbf{c}_{V_i}(t)-\mathbf{c}_{V_i}(t_k^i)).\end{aligned}$$

Using the definition of $\mathrm{sat}_{\frac{v}{\kappa}}(\cdot)$ one obtains that

$$\begin{aligned}\frac{d\mathcal{H}(\mathbb{P}(t))}{dt} \leq& -2\kappa\sum_{i=1}^N m_{V_i}(t)\Big(\|\mathbf{p}_i(t)-\mathbf{c}_{V_i}(t)\|^2 \\ &- \|\mathbf{p}_i(t)-\mathbf{c}_{V_i}(t)\|\left\|\mathbf{c}_{V_i}(t)-\mathbf{c}_{V_i}(t_k^i)\right\|\Big)\end{aligned}$$

if $\left\|\mathbf{p}_i(t)-\mathbf{c}_{V_i}(t_k^i)\right\| \leq v/\kappa$ and

$$\begin{aligned}\frac{d\mathcal{H}(\mathbb{P}(t))}{dt} \leq& 2v\sum_{i=1}^N m_{V_i}(t)\Bigg[\frac{-\|\mathbf{p}_i(t)-\mathbf{c}_{V_i}(t)\|^2}{\left\|\mathbf{p}_i(t)-\mathbf{c}_{V_i}(t_k^i)\right\|} \\ &+ \frac{\|\mathbf{p}_i(t)-\mathbf{c}_{V_i}(t)\|\left\|\mathbf{c}_{V_i}(t)-\mathbf{c}_{V_i}(t_k^i)\right\|}{\left\|\mathbf{p}_i(t)-\mathbf{c}_{V_i}(t_k^i)\right\|}\Bigg]\end{aligned}$$

otherwise. Now, assume that Proposition 3 holds. This implies that there is a $\tau \in [\tau_{\min}, \tau_{\max}]$ such that $h(s) \leq 0\ \forall\ s \in [0,\tau]$. The latter further implies that

$$\begin{aligned}&\mathrm{dm}(dgV_i(t_k^i+s))\left(1-\frac{m_{gV_i}(t_k^i+s)}{m_{dgV_i}(t_k^i+s)}\right) \\ &\qquad \leq \min\left(\rho_{gV_i}(t_k^i+s), \frac{\delta}{2}\right) \leq \frac{\delta}{2}. \qquad (15)\end{aligned}$$

Consider now the term $\left\|\mathbf{c}_{V_i}(t)-\mathbf{c}_{V_i}(t_k^i)\right\|$. Recalling (6) and the above inequality, yields that that $\left\|\mathbf{c}_{V_i}(t)-\mathbf{c}_{V_i}(t_k^i)\right\| \leq \delta\ \ \forall t \in [t_k^i, t_k^i+s]$. Define $\hat{\delta}(t) = \min\{\delta, \max_{i\in\mathbb{N}}\left\|\mathbf{c}_{V_i}(t)-\mathbf{c}_{V_i}(t_k^i)\right\|\}$. Then, returning to $d\mathcal{H}(\mathbb{P}(t))/dt$ we have that

$$\frac{d\mathcal{H}(\mathbb{P})}{dt} \leq -2\kappa\sum_{i=1}^N m_{V_i}\|\mathbf{p}_i-\mathbf{c}_{V_i}\|\left(\|\mathbf{p}_i-\mathbf{c}_{V_i}\|-\hat{\delta}\right),$$

if $\left\|\mathbf{p}_i-\mathbf{c}_{V_i}(t_k^i)\right\| \leq v/\kappa$ and

$$\frac{d\mathcal{H}(\mathbb{P})}{dt} \leq -2v\sum_{i=1}^N m_{V_i}\frac{\|\mathbf{p}_i-\mathbf{c}_{V_i}\|}{\left\|\mathbf{p}_i-\mathbf{c}_{V_i}(t_k^i)\right\|}\left(\|\mathbf{p}_i-\mathbf{c}_{V_i}\|-\hat{\delta}\right)$$

otherwise, where we have omitted the current time t argument to avoid cluttering of equations. The latter further implies that $d\mathcal{H}(\mathbb{P})/dt < 0$ for all $\sum_{i=1}^N \|\mathbf{p}_i-\mathbf{c}_{V_i}\| > N\hat{\delta}$, which in turns implies that $\mathcal{H}(\mathbb{P})$ is monotonically decreasing if $\|\mathbf{p}_i-\mathbf{c}_{V_i}\| > N\hat{\delta}$ for all $i\in\mathbb{N}$, and the proof is complete. ■

The above proposition establishes that the locational cost function monotonically decreases whenever the distance between the agent and its Voronoi centroid is equal or larger than $N\hat{\delta}$, which is a distance proportional to the data-sampled centroid error. As it will be shown in simulations and experiments in Section V and VI, $\mathcal{H}(\mathbb{P}(t))$ tends to be monotonically decreasing everywhere and the agents tend to converge to a CVT. This is the case whenever the error between the data-sampled centroid and true centroid converges to zero.

Corollary 2: If $\left\|\mathbf{c}_{V_i}(t)-\mathbf{c}_{V_i}(t_k^i)\right\| \to 0\ \forall\ i\in\mathbb{N}$, then $\mathbb{P}(t)$ converges asymptotically to a CVT.

Proof: Assume that $\left\|\mathbf{c}_{V_i}(t)-\mathbf{c}_{V_i}(t_k^i)\right\| \to 0\ \forall\ i\in\mathbb{N}$. Then, $\hat{\delta}(t)\to 0$ and one obtains that $d\mathcal{H}(\mathbb{P}(t))/dt < 0$ for all $\mathbf{p}_i(t) \neq \mathbf{c}_{V_i}(t)$ and zero otherwise. Using LaSalle's Invariance Principle and similar arguments as in [8, Proposition 3.1], one can conclude that $\mathbb{P}(t)$ converges to one of the centroidal configurations of $\mathbb{Q}$. ■

Remark 3: Corollary 2 can only guarantee asymptotic convergence to a CVT if the data-sampled centroid error converges to zero. Otherwise, one can only show the monotonic decrease of $\mathcal{H}(\mathbb{P}(t))$ outside a neighborhood around the centroids denoted as $\mathcal{B}[\mathbf{c}_{V_i}(t), N\hat{\delta}(t)] \subseteq \mathcal{B}[\mathbf{c}_{V_i}(t), N\delta]$. However, in practice, as will be shown in Sections V and VI, asymptotic convergence to a CVT seems to be always the case.

Note that as the agents approach their Voronoi centroids, their velocities tend to decrease, which in turn means that changes in the Voronoi cells start to slow down. The latter implies that the Voronoi centroids will also settle and the error between the true centroid and the data-sampled centroid will become smaller over time.

Remark 4: It is worth mentioning that, in contrast to previous work [30] and [33], the proposed triggering strategy tends to relax (or increase) the sensing intervals when the sensor network converges to a CVT or, alternatively, when $\left\|\mathbf{c}_{V_i}(t) - \mathbf{c}_{V_i}(t_k^i)\right\| \to 0 \ \forall \ i \in \mathbb{N}$. This is a consequence of the construction of the triggering function (8), which triggers a new sample when the upper bound on the distance between the data-sampled centroid and the true centroid exceeds a positive distance δ or exceeds the shortest distance between the centroid and the boundary of the agent's guaranteed Voronoi cell, i.e., $\rho_{gV_i}(t)$. As the sensor network converges to a CVT, the error becomes smaller satisfying, in general, the triggering condition for larger values of τ. Take for example the behavior of $\rho_{gV_i}(t+\tau)$ in (8). If we assume, for simplicity, an uniform density function, then we have that the agents will distribute themselves more evenly across the space with Voronoi cells of similar size and with their centroids close to the geometric center of their Voronoi cells. The latter will imply larger values of $\rho_{gV_i}(t+\tau)$ since the distance between the Voronoi boundary and the centroid is maximized. Larger value of $\rho_{gV_i}(t+\tau)$ will then translate to larger values of τ for which (8) will hold.

V. Simulations

The proposed self-triggered coverage control strategy is validated in both simulations and real robotic implementations with ground mobile agents. Based on the analysis in the previous sections, one can conclude about the effects of choosing key design parameters, i.e., δ, $\tau_{\min}$, and $\tau_{\max}$. A small δ will result in small sensing intervals (high sensing frequency) for a workspace $\mathbb{Q}$ and a velocity bound v, where the value of v is physically constrained by the dynamic capability of agents. As the proposed algorithm intends to reduce the cost of high sensing frequency, a relatively large δ is preferred. On the other hand, an extremely large value of δ will not be problematic since the sensing trigger condition (8) is limited by the minimum value between $\rho_{gV_i}(t_k^i + s)$ and $\frac{\delta}{2}$. In the simulations and experiments, we can approximately choose the value of δ based on the size of workspace and the number of agents and set a $\tau_{\min}$ mainly to conform with the hardware system computational constraints. Besides, the choice of $\tau_{\max}$ is not strict, but a small value of $\tau_{\max}$ (close to $\tau_{\min}$) will make the algorithm like a periodic one, and a larger $\tau_{\max}$ will result in a slow convergence to a CVT.

In this section, we present the results for eight different simulations involving large numbers of robots over a large-scale domain with an uniform distribution density function. The size of the workspace $\mathbb{Q}$ is assumed to be 4506 [m] $\times$ 3218 [m] (2.8 [miles] $\times$ 2 [miles]). The motion of the agents are modeled as in (1) with control law (5), where κ is chosen as 1. All other control parameters, such as velocity v and δ, varied according to Table I. The minimum sensing (or communication) interval for all cases is chosen as $\tau_{\min} = 0.033$ [s], which would correspond to a constant sensing frequency of 30 [Hz] if the coverage control algorithm is to be implemented in a periodic manner. For basis of comparison, we will compare our proposed self-triggered strategy with that of a periodic implementation executed every $\tau_{\min}$.

Table I also lists the resultant average sensing intervals $\bar{\tau}$ for each case, where it can be noted that the average value ranged from 4.1402 [s] to 36.5375 [s]. That corresponds to an average sampling frequency between 0.027 to 0.242 [Hz], representing a significant reduction of two to three orders of magnitude in the sensing (or communication) frequency of nearby agents when compared to a periodic implementation at 30 [Hz]. This suggests that a robot working on a large-scale environment can operate for longer periods of time without requiring other agents' information, saving on-board energy otherwise consumed by communication and sensing devices and reducing the burden of information exchange. For instance, if the power consumed by localization sensors or communication devices is assumed to be linearly proportional to the time the sensor is active or the device is transmitting [24], [41], then the use of the proposed strategy represents a reduction in power of nearly two to three orders of magnitude. In addition, note that $\bar{\tau}$ decreases if the number of agents or the maximum velocity increases. This observation is supported by the triggering condition in (8), which is a function of the guaranteed and dual guaranteed Voronoi cells. These cells are, in turn, a function of the number of agents and maximum velocity. That is, the Voronoi cells are smaller in average if the number of agents is larger and the guaranteed and dual guaranteed Voronoi cells decrease and increase in size, respectively, as a function of the maximum velocity. Furthermore, $\bar{\tau}$ increases nearly proportional to δ, which can be also expected from (8).

For illustration purposes, Fig. 3 shows the results for case 6 in Table I. The simulation of 100 robots with the Voronoi tessellation and the guaranteed Voronoi tessellation of the domain of interest are illustrated in Fig. 3(a). The aggregate errors of $\sum_{i=1}^{N} \left\|\mathbf{c}_{V_i}(t) - \mathbf{c}_{V_i}(t_k^i)\right\|$ and $\sum_{i=1}^{N} \left\|\mathbf{p}_i(t) - \mathbf{c}_{V_i}(t_k^i)\right\|$ with respect to time t are shown in Fig. 3(b). It can be noted from the zoomed-in portion in the plot that the two aggregate errors between $t = 960$ [s] and $t = 1000$ [s] fall into the scope of $\times 10^{-10}$ [m] (i.e., $\times 10^{-12}$ [m] per robot). Moreover, both aggregate errors eventually decay to zero, which suggests that the CVT configuration is achieved. The locational costs of the proposed self-triggered algorithm

Case	N	v [m/s]	δ [m]	$\tau_{\min}$ [s]	$\tau_{\max}$ [s]	$\bar{\tau}$ [s]
1	20	2.2352	300	0.033	150	14.6315
2	50	2.2352	150	0.033	75	7.1730
3	100	2.2352	75	0.033	40	4.1402
4	20	0.8941	300	0.033	150	36.5375
5	50	0.8941	150	0.033	75	18.3239
6	100	0.8941	75	0.033	40	10.1883
7	100	0.8941	150	0.033	75	18.2459
8	100	0.8941	300	0.033	150	35.2812

TABLE I: Simulation Parameters and Results.

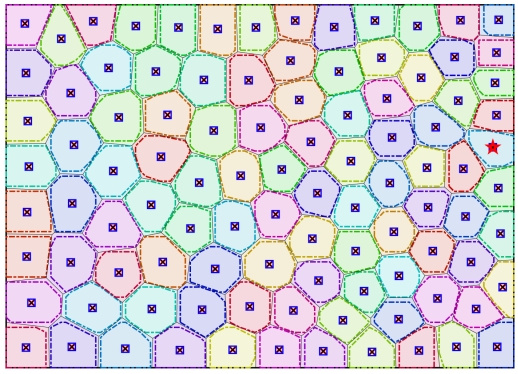

(a) Final Configuration of 100 Robots

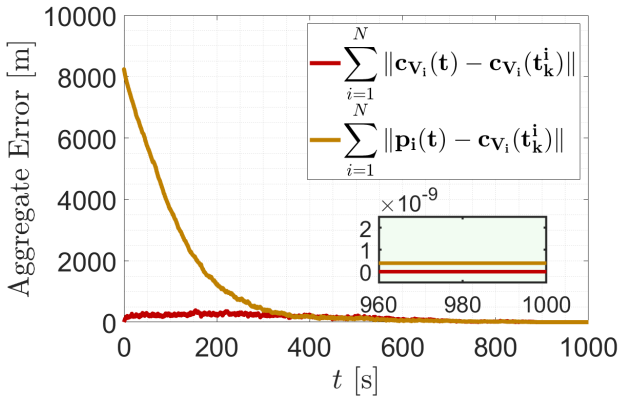

(b) Aggregate Errors

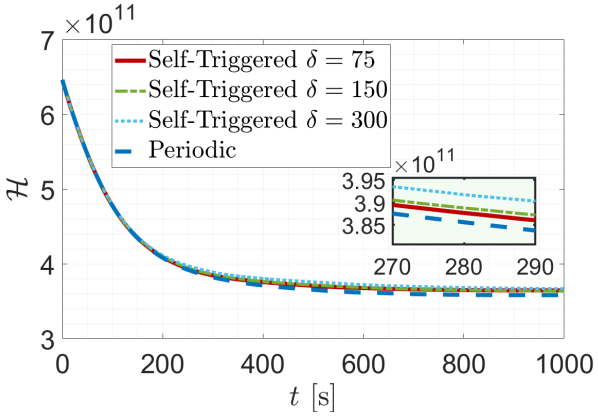

(c) Locational Cost

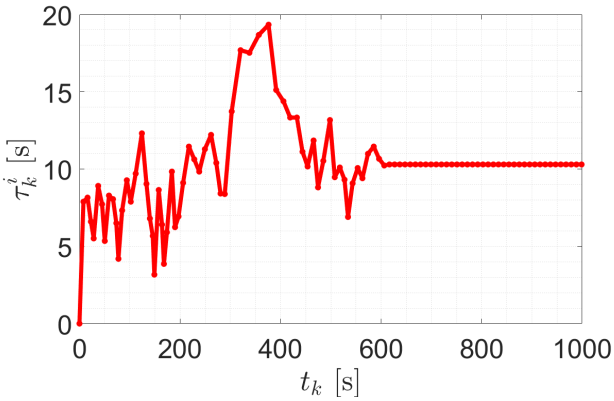

(d) Sensing Intervals

Fig. 3: A total of 100 robots are used to perform the proposed self-triggered coverage strategy in simulation. (a) Illustration of Voronoi tessellation and guaranteed Voronoi tessellation of 100 robots; (b) Profile of aggregate errors $\sum_{i=1}^{N} \left\|\mathbf{c}_{V_i}(t) - \mathbf{c}_{V_i}(t_k^i)\right\|$ and $\sum_{i=1}^{N} \left\|\mathbf{p}_i(t) - \mathbf{c}_{V_i}(t_k^i)\right\|$ versus time t [s]; (c) Profile of locational cost versus time t [s]; (d) Profile of one robot's (the one marked by a star symbol in (a)) updating interval τ_k^i versus updating time.

with $\delta = 75$ [m], 150 [m], and 300 [m] and a periodic implementation with constant updating interval of 0.033 [s] are compared in Fig. 3(c). It can be seen that the locational costs of both implementations approach a minimum value and that the behavior of the proposed self-triggered control is very similar to the periodic implementation. Furthermore, for small values of δ, the behavior of the proposed self-triggered algorithm gets closer to the periodic one. Finally, the sensing (or communication) instants for the first robot (marked by a red star sign in Fig. 3(a)) is recorded and plotted in Fig. 3(d). As one can see, the sensing intervals approach a constant value once the mobile sensor configuration is near a CVT.

VI. Experiments

In this section, we provide experimental results carried out on a group of ground mobile robots to illustrate the performance of the proposed algorithm in a real-world setting. The algorithms are implemented in *MATLAB* and the multi-robot team includes up to 9 *Khepera IV* differential-drive mobile robots. The real-time pose information of the multi-robot system is streamed from a motion capture system consisting of 8 *Vicon Vantage V8* cameras. The Voronoi regions are visualized on the workspace by an overhead projector. The robot working domain is a 5.182 [m] $\times$ 3.658 [m] (17 [feet] $\times$ 12 [feet]) rectangular space.

The kinematic equations of the Khepera IV vehicle can be modeled as

$$\begin{aligned}\dot{x}_i(t) =& \nu_i(t)\cos\psi_i(t),\\ \dot{y}_i(t) =& \nu_i(t)\sin\psi_i(t),\\ \dot{\psi}_i(t) =& \omega_i(t),\end{aligned}$$

where $\mathbf{p}_i(t) = [x_i(t), y_i(t)]^T$ is the Cartesian center of the robot, $\psi_i(t)$ is the heading, and $\nu_i(t)$ and $\omega_i(t)$ are the linear and angular velocity inputs, respectively. To transform the proposed saturated Cartesian velocity control law (5) into linear and angular velocity inputs, we used the following output feedback linearization control law

$$\begin{bmatrix}\nu_i(t)\\ \omega_i(t)\end{bmatrix} = \begin{bmatrix}\cos\psi_i(t) & \sin\psi_i(t)\\ -\frac{1}{L}\sin\psi_i(t) & \frac{1}{L}\cos\psi_i(t)\end{bmatrix}\mathbf{u}_i(t)$$

where $L = 0.14$ [m] is a control parameter. The above control input transformation [42] can effectively stabilize the agents with a small bounded errors. In addition, it is easy to show that the above transformation does not violate the agents maximum velocity constraint.

A total of 18 experiments are conducted with different initial configurations, density functions, number of robots, and control parameters. The list of parameters along with the average resultant sensing time intervals are summarized in Table II. The illustration of three different initial configurations for $N = 3$, $N = 6$, and $N = 9$ robots are also shown in Fig. 4 and 5. In brief, initial configuration 1 separates the robotic team into two groups and places the groups on two extreme sides of the space; initial configuration 2 deploys the multi-robot system in the middle of the space; and initial configuration 3 starts the robotic team on the left side of the working space. The maximum velocity for each agent is limited to $v = 0.1$ [m/s], the proportional control gain is chosen as $\kappa = 1$, and the time intervals limits are bounded by $\tau_{\text{min}} = 0.1$ [s] and $\tau_{\text{max}} = 5$ [s], where $\tau_{\min}$ represents the shortest allowable interval due to hardware, computational, and communication constraints.

As shown in Table II, the proposed control strategy is tested by using three different initial configurations, two different density functions (uniform and Gaussian), and three different δ values. Overall, the average sensing or communication interval ranged from 0.6590 to 2.5103 [s], which is about 6 to 25 times larger that the 0.1 [s] period that a periodic implementation would typically require. Note that $\bar{\tau}$ decreases as the number of robots increases, that is, a crowded workspace implies smaller Voronoi regions, which in turn requires more frequent updates. Similarly, a Gaussian distribution density function implies a CVT more concentrated towards the center of the space and, therefore, the resulting smaller average sampling intervals for scenario #4 when compared to a similar scenario #2. Moreover, the sensing intervals is nearly proportional to δ when the number of agents is small. Larger δ values provide greater tolerance to position uncertainties (as it can be inferred from (8b)) which in turns leads to generally larger sampling intervals. Furthermore, as seen in Fig. 4 and 5, which summarize the motion of the agents under the three different initial configurations assuming an uniform density function and control parameter $\delta = 1$ [m] (i.e., experimental scenarios 2, 5, and 6 in Table II), all the agent configurations eventually converge to a CVT despite the irregular updates intervals.

Sequential snapshots of experimental scenario #5 for $N = 9$ are presented in Fig. 6. As can be seen from the plots, the agents eventually converge to the centroids of the Voronoi cells. Fig. 7 illustrates the aggregate errors, the locational cost, and the sensing intervals for the same scenario. Note that the aggregate error between the real-time centroids and centroids at sensing instants t_k^i and the aggregate error between agents' positions and centroids at t_k^i approach very small values (about 0.000568 [m] and 0.0032 [m] per robot, respectively). Fig. 7(b) compares the evolution of the locational cost for the proposed self-triggered control and the 10 [Hz] periodic implementation. One can observe that both implementations minimize the locational cost and that the behavior of the self-triggered strategy approaches the evolution of the periodic implementation. Finally, the sensing (or communication) intervals for all nine agents as a function of time are presented in Fig. 7(c). Note that, in general, the sensing intervals are much larger than $\tau_{\min} = 0.1$ [s] and that they approach a constant value once the robotic team reaches a CVT. Fluctuations of intervals can be attributed to disturbance such as data streaming lags, the vehicles' nonholonomic constraints, and sensing errors. Differences in steady-state values are mostly due to the difference in size and shape of Voronoi cells and number of neighbors. Agents with more number of neighbors tend to yield smaller sensing intervals.

Exp. Scenario	Initial Config.	ϕ	δ [m]	$\bar{\tau}$ [s]		
				$N = 3$	$N = 6$	$N = 9$
#1	1	Uniform	0.5	0.8519	0.6626	0.6590
#2	1	Uniform	1	1.6515	1.3546	1.2205
#3	1	Uniform	1.5	2.5103	1.8858	1.3485
#4	1	Gaussian	1	1.3350	1.2157	1.1118
#5	2	Uniform	1	1.6254	1.3602	1.3104
#6	3	Uniform	1	1.2272	1.2808	1.0529

TABLE II: Experiment Parameters and Results.

VII. Conclusions

This paper presented a distributed, asynchronous self-triggered coverage control policy that is shown to locally optimize the position of an arbitrarily large group of mobile sensors while reducing the sensing or communication frequency among neighbors. The control strategy is a saturated, sampled-data version of Lloyd's algorithm and exploits the use of guaranteed and dual guaranteed Voronoi regions to determine when the agents need new knowledge of their neighbors positions. We proved that the control policy distributively minimizes a locational cost function while increasing the size of the sampling or communication intervals. The reduction of the communication or sampling frequency can lessen the burden on the communication network and prolong the lifespan of the sensors' energy resources. We also proved that the sampling intervals are positive and lower bounded, which is required for digital implementation.

Simulations with up to 100 agents and experiments with up to 9 ground vehicles illustrated the performance of the proposed coverage control strategy. They showed that the mobile sensor network converges to a CVT and that the sensing (or communication) intervals tend to stabilize at a large value when the robotic team motion settles. Furthermore, the results showed that the decay of the locational cost function using the proposed self-triggered strategy is very similar to the performance of a periodic (or continuous) implementation of the coverage control algorithm. In addition, the results showed an inverse relationship between the average sensing intervals and the density of agents and their maximum velocity. That is, the average sensing interval decreases with either an increase of the number of agents per area or their maximum velocity. Similarly, the sensing intervals have a nearly proportional relationship with the triggering control parameter δ. Larger δ

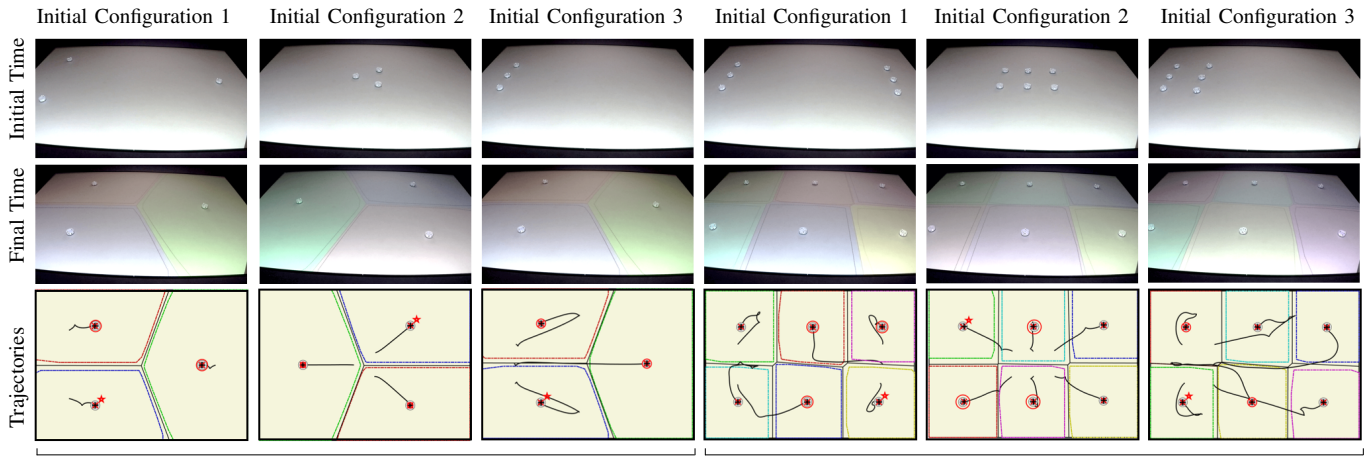

(a) $N = 3$ (b) $N = 6$

Fig. 4: Experimental results with $N = 3$ (first three columns) and $N = 6$ (last three columns) robots under three different initial configurations with uniform distribution density function and $\delta = 1$ [m]. The first row introduces the initial configurations while the second row contains the resulting final mobile sensor configurations illustrating the Voronoi cells. The third row depicts the trajectories of the agents under the three configurations. The red star marks the cell for the first agent, the black lines denote their trajectories, and the red circles the position uncertainties of nearby agents as seen from the first agent.

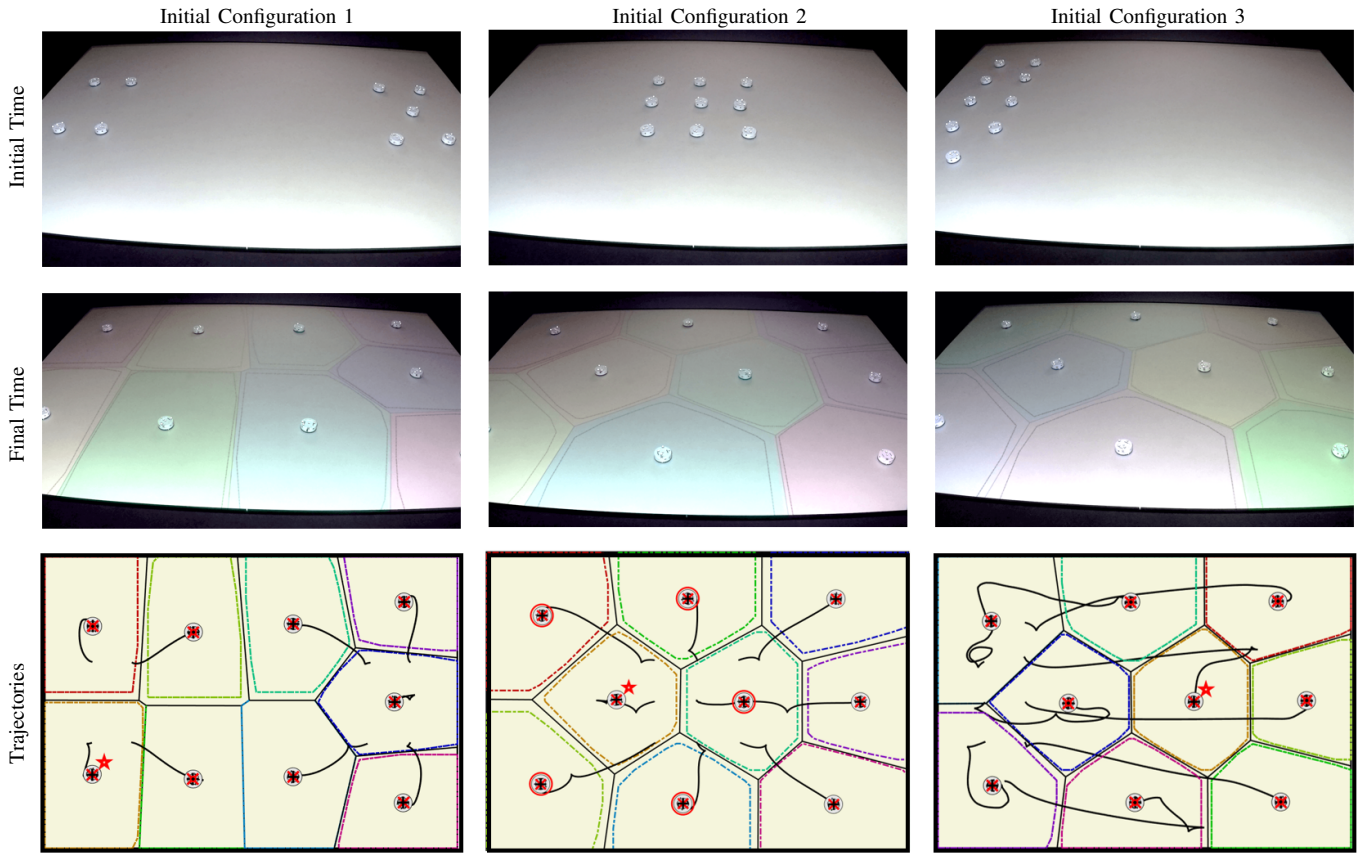

Fig. 5: Experimental results with $N = 9$ robots under three different initial configurations with uniform distribution density function and and $\delta = 1.0$ [m]. The first row introduces the initial configurations while the second row contains the resulting final mobile sensor configurations illustrating the Voronoi cells. The third row depicts the trajectories of the nine agents. The red star marks the cell for the first agent, the black lines trace their trajectories, and the small red circles within the squares denote the position uncertainties of agents 2 through 9 as seen from the first agent.

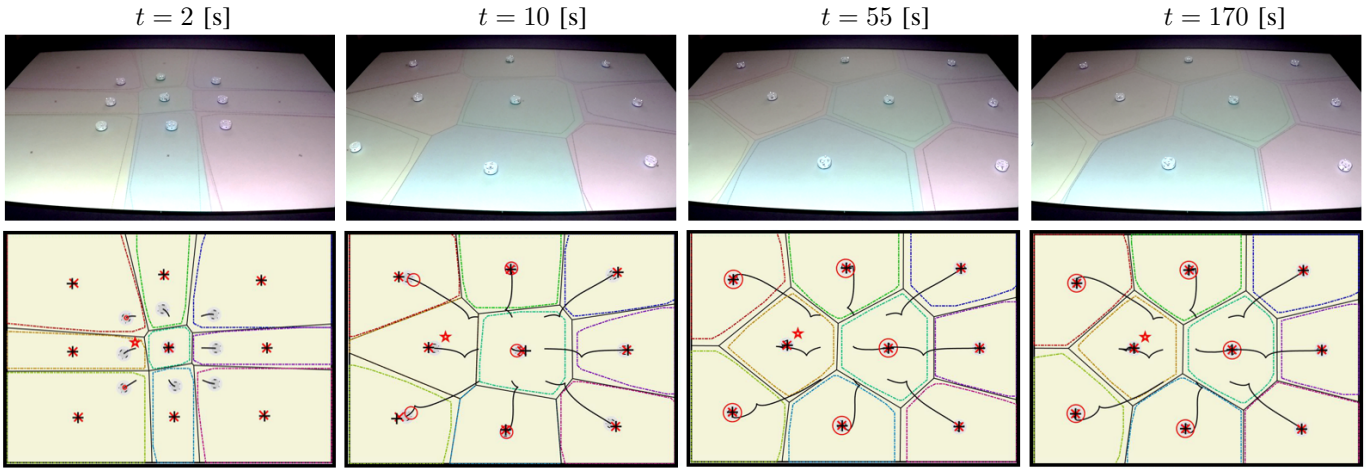

Fig. 6: Results for experimental scenario #5 with $N = 9$ robots. The first row contains the snapshots of the robotic implementation at $t = 2$, $t = 10$, $t = 55$, and $t = 170$ [s] where the standard and guaranteed Voronoi tessellations are visualized by an over-head projector. The second row includes the synchronous virtual illustrations of the experiment. In the virtual projections, the circles indicate the uncertainty about the positions of neighbors from the first agent's perspective (the one marked by a star symbol), the black lines the trajectories, and the red 'x' and black '+' denote the centroids at t_k^i and t, respectively.

values lead to larger sensing intervals at the expense of slower convergence rate.

Appendix
Mass Change Rates of Guaranteed and Dual Guaranteed Voronoi Regions

In this section we introduce bounds on the rate of change of mass for the guaranteed and dual guaranteed Voronoi regions.

Lemma 2: Let $\|\dot{\mathbf{p}}_i\| \leq v \ \forall \ t \geq t_k^i, \ i \in \mathbb{N}$. Assume that $\left\|\mathbf{p}_i(t_k^i) - \mathbf{p}_j(t_k^i)\right\| > \epsilon$ for some $\epsilon > 0$ and $\forall \ j \in \mathbb{N}_i(t_k^i)$ and pick $\tau \in (0, \frac{\epsilon}{2v})$. Then, $\|\dot{m}_{gV_i}(t)\|$ and $\|\dot{m}_{dgV_i}(t)\|$ are bounded for all $t \in [t_k^i, t_k^i + \tau]$.

Proof: First, consider (3) for $S = gV_i(t)$ and let $\tau = t - t_k^i < \frac{\epsilon}{2v}$. Define $\mathbf{Z}_i(t) := \{\mathbf{p}_i(t), \mathbf{z}_{i1}(t), \mathbf{z}_{i2}(t), \cdots\}$ as the set of generators for $gV_i(t)$, i.e., $\mathbf{z}_{i\ell} = \min_{\mathbf{x} \in \mathbb{X}_i(t)} \left\|\mathbf{x} - \mathbf{q}^\ell\right\|$ for some $\mathbf{q}^\ell \in \partial gV_i(t)$. Taking the time derivative and applying Leibniz Integral Rule [10], one can show that

$$\begin{aligned}
\dot{m}_{gV_i}(t) &= \int_{\partial gV_i(t)} \phi(\mathbf{q}) \hat{\mathbf{n}}^T(\mathbf{q}) \frac{\partial \mathbf{q}}{\partial \mathbf{Z}_i(t)} d\mathbf{q} \cdot \frac{d\mathbf{Z}_i(t)}{dt} \\
&= \sum_{\mathbf{z}_{i\ell} \in \mathbf{Z}_i(t)} \int_{\partial gV_{i\ell}(t)} \phi(\mathbf{q}) \hat{\mathbf{n}}^T(\mathbf{q}) \frac{\partial \mathbf{q}}{\partial \mathbf{p}_i(t)} d\mathbf{q} \cdot \frac{d\mathbf{p}_i(t)}{dt} \\
&\quad - \sum_{\mathbf{z}_{i\ell} \in \mathbf{Z}_i(t)} \int_{\partial gV_{i\ell}(t)} \phi(\mathbf{q}) \hat{\mathbf{n}}^T(\mathbf{q}) \frac{\partial \mathbf{q}}{\partial \mathbf{z}_{i\ell}(t)} d\mathbf{q} \cdot \frac{d\mathbf{z}_{i\ell}(t)}{dt}
\end{aligned} \tag{16}$$

where $\hat{\mathbf{n}}(\mathbf{q})$ is the unit outward normal vector, $\partial \mathbf{q}/\partial \mathbf{Z}_i(t)$ is the derivative of the boundary points with respect to $\mathbf{Z}_i(t)$, $d\mathbf{Z}_i(t)/dt$ is the velocity of the generator points, and $\partial gV_{i\ell}(t)$ is the boundary shared between $\mathbf{p}_i(t)$ and $\mathbf{z}_{i\ell}(t)$. The norm of the derivative of the boundary points is shown in [43], [44] to be given by

$$\left\|\frac{\partial \mathbf{q}}{\partial \mathbf{z}_{i\ell}(t)}\right\| = \frac{\|\mathbf{q} - \mathbf{z}_{i\ell}(t)\|}{\|\mathbf{p}_i(t) - \mathbf{z}_{i\ell}(t)\|}, \quad \left\|\frac{\partial \mathbf{q}}{\partial \mathbf{p}_i(t)}\right\| = \frac{\|\mathbf{q} - \mathbf{p}_i(t)\|}{\|\mathbf{p}_i(t) - \mathbf{z}_{i\ell}(t)\|}.$$

Since at the boundary points, $\|\mathbf{q} - \mathbf{z}_{i\ell}(t)\| = \|\mathbf{q} - \mathbf{p}_i(t)\|$ and $\|\mathbf{p}_i(t) - \mathbf{z}_{i\ell}(t)\| = \left\|\mathbf{p}_i(t) - \mathbf{p}_j(t_k^i)\right\| - v\tau$ for some $j \in \mathbb{N}_i(t_k^i)$ (see [30]), one has that

$$\left\|\frac{\partial \mathbf{q}}{\partial \mathbf{z}_{i\ell}(t)}\right\| = \left\|\frac{\partial \mathbf{q}}{\partial \mathbf{p}_i(t)}\right\| = \frac{\|\mathbf{q} - \mathbf{p}_i(t)\|}{\left\|\mathbf{p}_i(t) - \mathbf{p}_j(t_k^i)\right\| - v\tau}.$$

Returning to (16) we have that

$$\begin{aligned}
\|\dot{m}_{gV_i}(t)\| &\leq \sum_{\mathbf{z}_{i\ell} \in \mathbf{Z}_i(t)} \int_{\partial gV_{i\ell}(t)} \phi(\mathbf{q}) \left\|\hat{\mathbf{n}}^T(\mathbf{q})\right\| \\
&\quad \cdot \left[\left\|\frac{\partial \mathbf{q}}{\partial \mathbf{p}_i(t)}\right\| \left\|\frac{d\mathbf{p}_i(t)}{dt}\right\| + \left\|\frac{\partial \mathbf{q}}{\partial \mathbf{z}_{i\ell}(t)}\right\| \left\|\frac{d\mathbf{z}_{i\ell}(t)}{dt}\right\|\right] d\mathbf{q} \\
&\leq 2\phi_{\max} \sum_{\mathbf{z}_{i\ell} \in \mathbf{Z}_i(t)} \int_{\partial gV_{i\ell}(t)} \frac{v \|\mathbf{q} - \mathbf{p}_i(t)\|}{\left\|\mathbf{p}_i(t) - \mathbf{p}_j(t_k^i)\right\| - v\tau} d\mathbf{q} \\
&\leq \frac{2\phi_{\max} v \sum_{\mathbf{z}_{i\ell} \in \mathbf{Z}(t)} \int_{\partial gV_{i\ell}(t)} \|\mathbf{q} - \mathbf{p}_i(t)\| \, d\mathbf{q}}{\min_{j \in \mathbb{N}_i(t_k^i)} \left\|\mathbf{p}_i(t) - \mathbf{p}_j(t_k^i)\right\| - v\tau}
\end{aligned} \tag{17}$$

where we used the fact that $\|\dot{\mathbf{p}}_i(t)\| \leq v$ and $\|\dot{\mathbf{z}}_{i\ell}(t)\| \leq v$. Now, from Proposition 2, we have that $gV_i(t_k^i + \tau) \subset V_i(t_k^i)$, therefore, $\|\mathbf{q} - \mathbf{p}_i(t)\| \leq \mathrm{dm}(gV_i(t)) \leq \mathrm{dm}(V_i(t_k^i))$. Returning to (17) we obtain

$$\begin{aligned}
\|\dot{m}_{gV_i}(t)\| &\leq \frac{2\phi_{\max} v \cdot \mathrm{dm}(V_i(t_k^i)) \sum_{\mathbf{z}_{i\ell} \in \mathbf{Z}_i(t)} \int_{\partial gV_{i\ell}(t)} d\mathbf{q}}{\min_{j \in \mathbb{N}_i(t_k^i)} \left\|\mathbf{p}_i(t) - \mathbf{p}_j(t_k^i)\right\| - v\tau} \\
&\leq \frac{2\phi_{\max} v \cdot \mathrm{dm}(V_i(t_k^i)) \sum_{\mathbf{z}_{i\ell} \in \mathbf{Z}_i(t)} \int_{\partial gV_{i\ell}(t)} d\mathbf{q}}{\min_{j \in \mathbb{N}_i(t_k^i)} \left\|\mathbf{p}_i(t_i^k) - \mathbf{p}_j(t_k^i)\right\| - 2v\tau} \\
&\leq \frac{2\phi_{\max} v}{\epsilon - 2v\tau} \mathrm{dm}(V_i(t_k^i)) \int_{\partial gV_i(t)} d\mathbf{q}.
\end{aligned}$$

Now, given that $gV_i(t)$ and $V_i(t_k^i)$ are convex and $gV_i(t) \subset V_i(t_k^i)$, one can bound $\int_{\partial gV_i(t)} d\mathbf{q} \leq \int_{V_i(t_k^i)} d\mathbf{q} \leq$

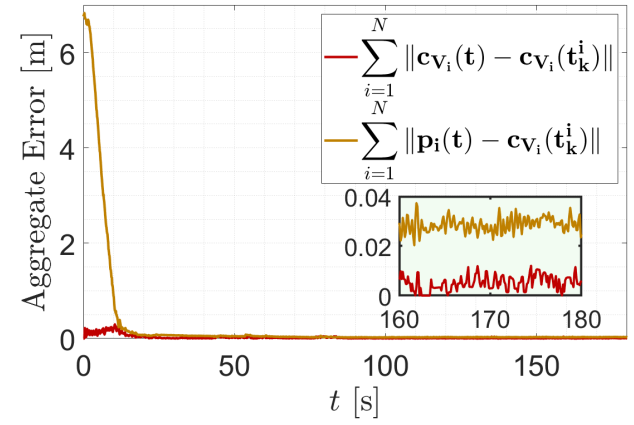

(a) Aggregate Errors

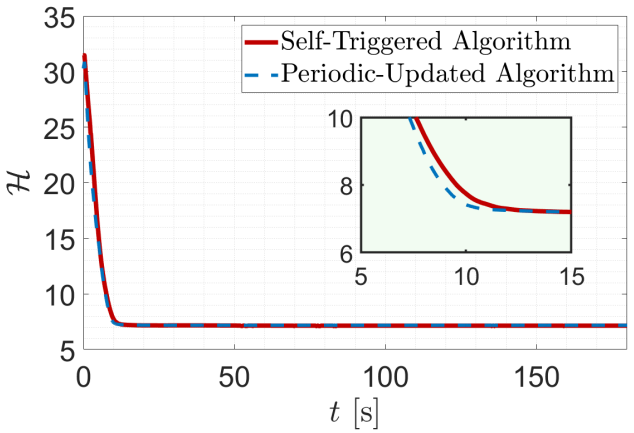

(b) Locational Cost

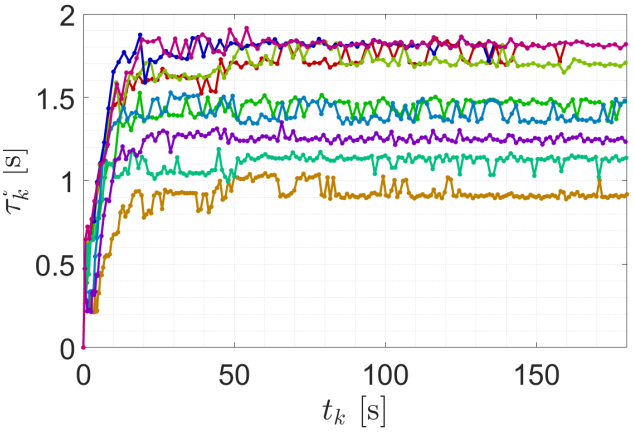

(c) Sensing Intervals

Fig. 7: Results for experimental Scenario #5 with $N = 9$ robots. (a) Profile of aggregate errors $\sum_{i=1}^{N} \left\|\mathbf{c}_{V_i}(t) - \mathbf{c}_{V_i}(t_k^i)\right\|$ and $\sum_{i=1}^{N} \left\|\mathbf{p}_i(t) - \mathbf{c}_{V_i}(t_k^i)\right\|$ versus time t [s]; (b) Profile of locational cost versus time t [s]; (c) Profile of multi-robot system's updating intervals τ_i^k versus updating time t_k [s].

$\mathcal{A}_n(\frac{1}{2}\mathrm{dm}(V_i(t_k^i)))$ and obtain that

$$\|\dot{m}_{gV_i}(t)\| \leq \frac{2\phi_{\max} v}{\epsilon - 2v\tau} \mathrm{dm}(V_i(t_k^i)) \mathcal{A}_n \left(\frac{1}{2}\mathrm{dm}(V_i(t_k^i))\right) \leq \frac{2\phi_{\max} v}{\epsilon - 2v\tau} \mathrm{dm}(\mathbb{Q}) \mathcal{A}_n \left(\frac{1}{2}\mathrm{dm}(\mathbb{Q})\right)$$

which is upper bounded for $\epsilon > 2v\tau$.

Now, consider (3) for $S = dgV_i(t)$ but assume that $\mathbf{Z}_i(t)$ are the generators of $dgV_i(t)$. Following similar arguments as for $m_{gV_i}(t)$, one can obtain similar to (17) that

$$\|\dot{m}_{dgV_i}(t)\| \leq \frac{2\phi_{\max} v}{\epsilon - 2v\tau} \sum_{\mathbf{z}_{i\ell} \in \mathbf{Z}_i(t)} \int_{\partial dgV_{i\ell}(t)} \|\mathbf{q} - \mathbf{p}_i(t)\| \, d\mathbf{q} \tag{18}$$

where $\|\mathbf{q} - \mathbf{p}_i(t)\| \leq \mathrm{dm}(\mathbb{Q})$. Note that $dgV_i(t)$ may not be convex, therefore, the integral cannot be easily bounded with the surface area of an n-dimensional ball. However, we have that the edges of $dgV_i(t)$, denoted as $\partial dgV_{ij}(t)\ \forall\ j \in \mathbb{N}_i(t_k^i)$, lie on the surface of the hyperboloid obtained by rotating the farthest hyperbola from $\mathbf{p}_i(t)$ with foci $\mathbf{p}_i(t)$ and $\mathbf{p}_j(t_k^i)$ and semi-major axis $v\tau/2$ [30], rotated about it semi-minor axis. Each surface of these hyperboloids can be bounded by the surface area of a half n-dimensional ball of radius radius $\frac{1}{2}\mathrm{dm}(\mathbb{Q})$. Therefore,

$$\sum_{\mathbf{z}_{i\ell} \in \mathbf{Z}_i(t)} \int_{\partial dgV_{i\ell}(t)} d\mathbf{q} = \sum_{j \in \mathbb{N}_i(t_k^i)} \int_{\partial dgV_{ij}(t)} d\mathbf{q} \leq \frac{1}{2}\mathcal{A}_n \left(\frac{1}{2}\mathrm{dm}(\mathbb{Q})\right) |\mathbb{N}_i(t_k^i)|$$

where $|\mathbb{N}_i(t_k^i)|$ denotes the cardinality of a set $\mathbb{N}_i(t_k^i)$, which is a bounded quantity. Note that the bound is, in general, extremely conservative. Now, returning to (18) one obtains

$$\|\dot{m}_{dgV_i}(t)\| \leq \frac{\phi_{\max} v}{\epsilon - 2v\tau} \mathrm{dm}(\mathbb{Q}) |\mathbb{N}_i(t_k^i)| \mathcal{A}_n \left(\frac{1}{2}\mathrm{dm}(\mathbb{Q})\right)$$

which is bounded for $\epsilon > 2v\tau$. ■

References

[1] I. Khoufi, P. Minet, A. Laouiti, and S. Mahfoudh, "Survey of deployment algorithms in wireless sensor networks: Coverage and connectivity issues and challenges," *International Journal of Autonomous and Adaptive Communications Systems*, vol. 10, no. 4, pp. 341–390, 2017.

[2] J. Gu, T. Su, Q. Wang, X. Du, and M. Guizani, "Multiple moving targets surveillance based on a cooperative network for multi-uav," *IEEE Communications Magazine*, vol. 56, no. 4, pp. 82–89, 2018.

[3] D. P. Agrawal, "Applications of sensor networks," in *Embedded Sensor Systems*. Singapore: Springer, 2017, pp. 35–63.

[4] D. He, S. Chan, and M. Guizani, "Drone-assisted public safety networks: The security aspect," *IEEE Communications Magazine*, vol. 55, no. 8, pp. 218–223, Aug 2017.

[5] L. Zhang, Z. Zhang, R. Siegwart, and J. J. Chung, "Distributed pdop coverage control: Providing large-scale positioning service using a multi-robot system," *IEEE Robotics and Automation Letters*, vol. 6, no. 2, pp. 2217–2224, 2021.

[6] L. Nguyen, S. Kodagoda, R. Ranasinghe, and G. Dissanayake, "Mobile robotic sensors for environmental monitoring using gaussian markov random field," *Robotica*, vol. 39, no. 5, pp. 862–884, 2021.

[7] A. V. Savkin, T. M. Cheng, Z. Xi, F. Javed, A. S. Matveev, and H. Nguyen, *Decentralized coverage control problems for mobile robotic sensor and actuator networks*. John Wiley & Sons, 2015.

[8] J. Cortés, S. Martínez, T. Karatas, and F. Bullo, "Coverage control for mobile sensing networks," *IEEE Transactions on Robotics and Automation*, vol. 20, no. 2, pp. 243–255, April 2004.

[9] M. Schwager, D. Rus, and J.-J. Slotine, "Decentralized, adaptive coverage control for networked robots," *The International Journal of Robotics Research*, vol. 28, no. 3, pp. 357–375, 2009.

[10] Y. Diaz-Mercado, S. G. Lee, and M. Egerstedt, "Human-swarm interactions via coverage of time-varying densities," in *Trends in Control and Decision-Making for Human–Robot Collaboration Systems*. Springer, 2017, pp. 357–385.

[11] M. Rout and R. Roy, "Dynamic deployment of randomly deployed mobile sensor nodes in the presence of obstacles," *Ad Hoc Networks*, vol. 46, pp. 12–22, 2016.
[12] P. F. Hokayem, D. Stipanović, and M. W. Spong, "Dynamic coverage control with limited communication," in *Proc. of American Control Conference*, July 2007, pp. 4878–4883.
[13] R. Yehoshua, N. Agmon, and G. A. Kaminka, "Robotic adversarial coverage of known environments," *The International Journal of Robotics Research*, vol. 35, no. 12, pp. 1419–1444, 2016.
[14] E. J. Rodríguez-Seda and Y. Diaz-Mercado, "Decentralized persistent area coverage control with loss of awareness," in *IEEE Conference on Control Technology and Applications*, 2020, pp. 528–535.
[15] Y. Wang and I. I. Hussein, "Awareness coverage control over large-scale domains with intermittent communications," *IEEE Transactions on Automatic Control*, vol. 55, no. 8, pp. 1850–1859, Aug 2010.
[16] C. Song, L. Liu, G. Feng, and S. Xu, "Optimal control for multi-agent persistent monitoring," *Automatica*, vol. 50, no. 6, pp. 1663 –1668, 2014.
[17] G. M. Atinç, D. M. Stipanović, and P. G. Voulgaris, "A swarm-based approach to dynamic coverage control of multi-agent systems," *Automatica*, vol. 112, p. 108637, 2020.
[18] O. Arslan, "Statistical coverage control of mobile sensor networks," *IEEE Transactions on Robotics*, vol. 35, no. 4, pp. 889–908, 2019.
[19] J. M. Palacios-Gasós, D. Tardioli, E. Montijano, and C. Sagüés, "Equitable persistent coverage of non-convex environments with graph-based planning," *The International Journal of Robotics Research*, vol. 38, no. 14, pp. 1674–1694, 2019.
[20] X. Xu, E. Rodríguez-Seda, and Y. Diaz-Mercado, "Persistent awareness-based multi-robot coverage control," in *Proc. IEEE Conference on Decision and Control*, Dec. 2020, pp. 5315–5320.
[21] J. R. Marden, G. Arslan, and J. S. Shamma, "Cooperative control and potential games," *IEEE Transactions on Systems, Man, and Cybernetics, Part B*, vol. 39, no. 6, pp. 1393–1407, 2009.
[22] S. Rahili, J. Lu, W. Ren, and U. M. Al-Saggaf, "Distributed coverage control of mobile sensor networks in unknown environment using game theory: Algorithms and experiments," *IEEE Transactions on Mobile Computing*, vol. 17, no. 6, pp. 1303–1313, 2018.
[23] Y. Kantaros and M. M. Zavlanos, "Distributed communication-aware coverage control by mobile sensor networks," *Automatica*, vol. 63, pp. 209–220, 2016.
[24] D. Baumann, F. Mager, M. Zimmerling, and S. Trimpe, "Control-guided communication: Efficient resource arbitration and allocation in multi-hop wireless control systems," *IEEE Control Systems Letters*, vol. 4, no. 1, pp. 127–132, 2019.
[25] P. Tabuada, "Event-triggered real-time scheduling of stabilizing control tasks," *IEEE Transactions on Automatic Control*, vol. 52, no. 9, pp. 1680–1685, 2007.
[26] W. P. M. H. Heemels, K. H. Johansson, and P. Tabuada, "An introduction to event-triggered and self-triggered control," in *Proc. of IEEE Conference on Decision and Control*, Dec 2012, pp. 3270–3285.
[27] M. Zhong and C. G. Cassandras, "Asynchronous distributed optimization with event-driven communication," *IEEE Transactions on Automatic Control*, vol. 55, no. 12, pp. 2735–2750, 2010.
[28] N. Hayashi, Y. Muranishi, and S. Takai, "Distributed event-triggered control for voronoi coverage," in *International Conference on Event-based Control, Communication, and Signal Processing*, 2015, pp. 1–4.
[29] E. J. Rodríguez-Seda, "Self-triggered reduced-attention output feedback control for linear networked control systems," *IEEE Transactions on Industrial Informatics*, vol. 15, no. 1, pp. 348–356, 2018.
[30] C. Nowzari and J. Cortés, "Self-triggered coordination of robotic networks for optimal deployment," *Automatica*, vol. 48, no. 6, pp. 1077–1087, 2012.
[31] C. Nowzari, J. Cortés, and G. J. Pappas, "Team-triggered coordination of robotic networks for optimal deployment," in *American Control Conference*, 2015, pp. 5744–5751.
[32] D. Tabatabai, M. Ajina, and C. Nowzari, "Self-triggered distributed k-order coverage control," *IEEE Transactions on Control of Network Systems*, 2021, in press.
[33] M. Ajina, D. Tabatabai, and C. Nowzari, "Asynchronous distributed event-triggered coordination for multiagent coverage control," *IEEE Transactions on cybernetics*, 2021, in press.
[34] W. Evans and J. Sember, "Guaranteed Voronoi diagrams of uncertain sites," in *Canadian Conference on Computational Geometry*, Dec. 2008, pp. 207–210.
[35] M. Mazo, A. Anta, and P. Tabuada, "An ISS self-triggered implementation of linear controllers," *Automatica*, vol. 46, no. 8, pp. 1310–1314, 2010.
[36] Q. Du, V. Faber, and M. Gunzburger, "Centroidal Voronoi tessellations: Applications and algorithms," *SIAM Review*, vol. 41, no. 4, pp. 637–676, 1999.
[37] J. Cortés, S. Martinez, T. Karatas, and F. Bullo, "Coverage control for mobile sensing networks: Variations on a theme," in *Mediterranean Conference on Control and Automation*, 2002, pp. 9–13.
[38] A. Okabe, B. Boots, K. Sugihara, and S. N. Chiu, *Spatial tessellations: Concepts and applications of Voronoi diagrams*. John Wiley & Sons, 2009.
[39] M. Emelianenko, L. Ju, and A. Rand, "Nondegeneracy and weak global convergence of the Lloyd algorithm in $\mathbb{R}^d$," *SIAM Journal on Numerical Analysis*, vol. 46, no. 3, pp. 1423–1441, 2008.
[40] D. M. Stipanović, C. J. Tomlin, and G. Leitmann, "Monotone approximations of minimum and maximum functions and multi-objective problems," *Applied Mathematics & Optimization*, vol. 66, no. 3, pp. 455–473, 2012.
[41] M. J. Miller and N. H. Vaidya, "Minimizing energy consumption in sensor networks using a wakeup radio," in *IEEE Wireless Communications and Networking Conference*, 2004, pp. 2335–2340.
[42] A. De Luca, G. Oriolo, and M. Vendittelli, "Control of wheeled mobile robots: An experimental overview," in *RAMSETE — Articulated and Mobile Robotics for Services and Technologies*, S. Nicosia, B. Siciliano, A. Bicchi, and P. Valigi, Eds. Springer-Verlag, 2001, pp. 181–226.
[43] Q. Du, M. Emelianenko, and L. Ju, "Convergence of the lloyd algorithm for computing centroidal voronoi tessellations," *SIAM Journal on Numerical Analysis*, vol. 44, no. 1, pp. 102–119, 2006.
[44] M. Santos, Y. Diaz-Mercado, and M. Egerstedt, "Coverage control for multirobot teams with heterogeneous sensing capabilities," *IEEE Robotics and Automation Letters*, vol. 3, no. 2, pp. 919–925, 2018.

Erick J. Rodríguez-Seda received the B.S. degree in electrical engineering from the University of Puerto Rico, Mayagüez, in 2004 and the M.S. and Ph.D. degrees in electrical and computer engineering from the University of Illinois, Urbana-Champaign, in 2007 and 2011, respectively. He is currently an Associate Professor with the Department of Weapons, Robotics, and Control Engineering at the United States Naval Academy. From 2011 to 2013, he was a Postdoctoral Research Associate at the University of Texas at Dallas. His current research interests include networked control, collision avoidance, multi-agent systems, and cybersecurity of control systems.

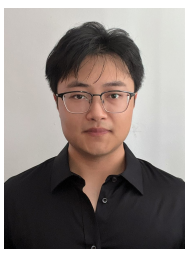

Xiaotian Xu received a B.S. degree in vehicle engineering from the Shandong University of Science and Technology, China, in 2015, and an M.S. degree in mechanical engineering from the Marshall University, WV, USA, in 2018. He is currently working toward a Ph.D. degree in mechanical engineering with the Collaborative Controls and Robotics Laboratory at the University of Maryland, MD, USA.

His research interests include distributed control and collaborative control of multi-robot and swarm systems.

Josep M. Olm received the M.Sc. and Ph.D. degrees in Physics from the University of Barcelona and the Universitat Politècnica de Catalunya, both in Barcelona, Spain, in 1989 and 2004, respectively.

Since 2003 he is with the Universitat Politècnica de Catalunya, where he is currently an Associate Professor at the Department of Mathematics and a researcher at the Institute of Industrial and Control Engineering. His research interests are in the field of control theory, including sliding, adaptive, repetitive, and complex networks control. He is author or co-author of 90 journal articles and conference papers, and one book.

Dr. Olm served as Associate Editor of the IEEE Transactions on Circuits and Systems-I: Regular papers for the term 2014-2015.

Arnau Dòria-Cerezo was born in Barcelona, Spain, in 1974. He received an undergraduate degree in electromechanical engineering and a Ph.D. degree in advanced automation and robotics from the Universitat Politècnica de Catalunya (UPC), Barcelona, in 2001 and 2006, respectively, and the D.E.A. degree in industrial automation from the Institut National des Sciences Appliqueés de Lyon, Villeurbanne, France, in 2001.

He is currently an Associate Professor with the Department of Electrical Engineering, UPC, and carries on his research activities with the Advanced Control of Energy Systems Group, at the Institute of Industrial and Control Engineering, UPC. From 2003 to 2004, he was a Control Training Site-Research Fellow with the Laboratoire des Signaux et Systèmes, Supélec, France. In 2010, he was a visitor at the Technische Universiteit Delft, Delft, The Netherlands. His research interests include modelling and control of electrical systems and automotive applications.

Since 2017, Dr. Dòria-Cerezo is an Associate Editor for Control Engineering Practice.

Yancy Diaz-Mercado (S'14–M'16) earned his Ph.D. degree in Electrical Engineering from the Georgia Institute of Technology in 2016, and M.S. degree in in Electrical Engineering from the same institution in 2014. He graduated with a B.S. degree in Electrical Engineering from the University of Puerto Rico at Mayagüez in 2011. From 2016 to 2018, he was a Senior Research Scientist with the Johns Hopkins University Applied Physics Laboratory, working on Advanced Concepts for Guidance, Navigation, and Controls applications.

In 2018, he joined the faculty of the Department of Mechanical Engineering at the University of Maryland, College Park as an Assistant Professor. He is the director of the Collaborative Controls and Robotics Laboratory, whose research focus is on developing collaborative autonomy for multi-agent systems, robotics, and enabling human-swarm interactions using notions from optimal control, nonlinear control, and graph theory. He is a member of the Maryland Robotics Center, and has several accolades for his work on swarm robotics including keynotes and patents.